Methods to label, image, and analyze the complex structural architectures of microvascular networks

Bruce A. Corliss 🆔 | Corbin Mathews | Richard Doty | Gustavo Rohde | Shayn M. Peirce

Department of Biomedical Engineering, University of Virginia, Charlottesville, Virginia

Correspondence
Bruce A. Corliss, Department of Biomedical Engineering, University of Virginia, Charlottesville, VA.
Email: bac7wj@virginia.edu

Abstract

Microvascular networks play key roles in oxygen transport and nutrient delivery to meet the varied and dynamic metabolic needs of different tissues throughout the body, and their spatial architectures of interconnected blood vessel segments are highly complex. Moreover, functional adaptations of the microcirculation enabled by structural adaptations in microvascular network architecture are required for development, wound healing, and often invoked in disease conditions, including the top eight causes of death in the Unites States. Effective characterization of microvascular network architectures is not only limited by the available techniques to visualize microvessels but also reliant on the available quantitative metrics that accurately delineate between spatial patterns in altered networks. In this review, we survey models used for studying the microvasculature, methods to label and image microvessels, and the metrics and software packages used to quantify microvascular networks. These programs have provided researchers with invaluable tools, yet we estimate that they have collectively attained low adoption rates, possibly due to limitations with basic validation, segmentation performance, and nonstandard sets of quantification metrics. To address these existing constraints, we discuss opportunities to improve effectiveness, rigor, and reproducibility of microvascular network quantification to better serve the current and future needs of microvascular research.

KEYWORDS
blood vessels, image analysis, image quantification, microvasculature, vascular network, vessel architecture

1 | INTRODUCTION

The microvasculature plays a plethora of key roles in maintaining tissue homeostasis, including modulating oxygen transport,[1] nutrient delivery, inflammation response,[2] and wound healing.[3] Structural changes to the microvascular architecture have been shown to profoundly regulate these fundamental biologic processes.[4] Therefore, characterization of the complex changes in spatial structure of the microvascular architecture gives a better understanding of the roles microvessels play in pathogenesis, maintenance, prevention, and amelioration of diseases. Indeed, the importance of the microvasculature has long been appreciated in diseases such as small vessel disease,[5] coronary microvascular disease,[6] and the abundance of complications associated with diabetes.[7] However, recent research has indicated that the microvasculature also plays key roles in the top eight causes of death in the United States[8] (Figure 1) and many others, including (1) heart disease: impaired infarct wound healing,[9] reduced oxygenation,[10] pulmonary hypertension in pre-capillary and post-capillary vessels[11]; (2) cancer: pathological angiogenesis,[12] enriched microvessel permeability,[13] significant route for metastasis[14]; (3) lower respiratory disease: capillary dropout,[15] reduced muscle oxygenation,[16] airway rigidity from vasodilation[17]; (4) stroke: impaired microvascular flow patterns[18] and reduced oxygenation,[19] pericyte constriction of capillaries,[20] dropout of functioning capillaries[21]; (5) unintentional injuries: angiogenesis,[22] clot formation,[23] immune cell recruitment[24]; (6) Alzheimer's: attenuated vasodilation response,[25] amyloid angiopathy,[26] and tissue hypoxia[25]; (7) diabetes mellitus: capillary permeability, pericyte dropout, capillary dropout[27]; and (8) pneumonia and influenzas: capillary permability,[28] immune cell recruitment,[28] and impaired lung oxygen transport.[29] Additionally, the microvasculature is recognized as one of the most promising routes of drug delivery[30] by enabling direct targeting of microvascular endothelial cells with intravascularly injected drugs to exert profound therapeutic effects in disease conditions.[31] The overall import of the microvasculature in biomedical research is quickly approaching that of the nearly ubiquitous roles that the immune system plays in basic organismal processes[32,33] and disease development,[34] and future research focused on microvascular structure, function, and adaptations promises profound opportunities for curing human disease.

In this review, we highlight new key developments and survey contemporary and classical models of the microvasculature, along with techniques to label and image microvessels at high resolution where the complete microvascular structure is captured. Therefore, microvascular research that fails to resolve the smallest-sized vascular structures is omitted or given less emphasis, such as fundus imaging of the retina[35] and other clinical imaging methods. Although a subset of the modalities covered can yield 3D images, we focus on analysis of 2D projections of 3D vessel networks since it can be universally applied to all microvascular imaging modalities, 2D repres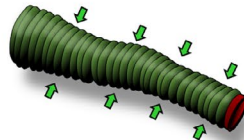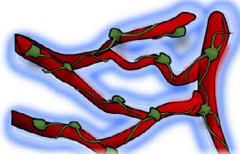entations of 3D networks retain much of their information,[36] and 2D methods for quantification of vessel architecture can be extended to three dimensions,[37] although we do comment on the potential pitfalls of using 2D metrics to characterize 3D microvascular structures. Furthermore, many of the 3D modalities for microvascular imaging have reduced axial resolution compared to lateral, and practical considerations of acquisition time usually lead to further reduced axial sampling.[38] The currently available programs to analyze and quantify microvascular structures are also covered, along with constructive proposals for improvement in this area. While each topic covered could be a detailed examination on its own, this review is meant to offer a basic orientation of the technological options available for microvascular research and a perspective on analytical techniques to increase scientific rigor as science faces an ongoing crisis in reproducibility.[39]
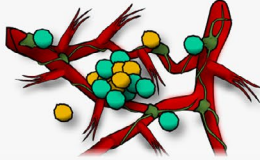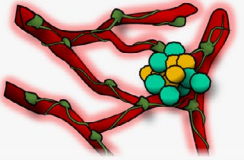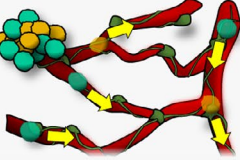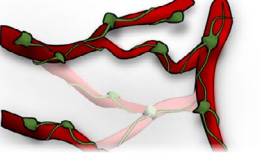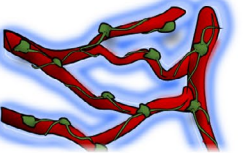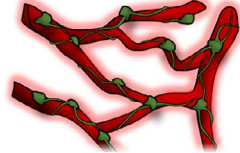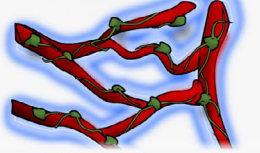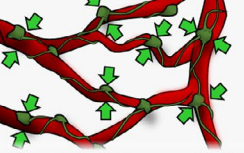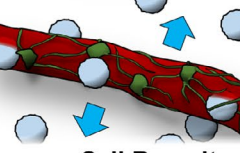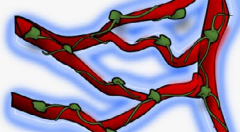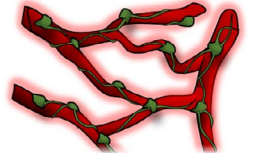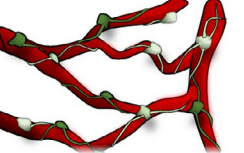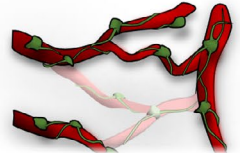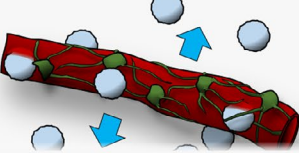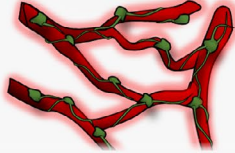
2 | MARKERS AND MODELS TO STUDY MICROVASCULAR NETWORK ARCHITECTURE

The study of the complex architecture of microvasculature requires proper labeling and visualization of microvessels, using either a marker for particular cell types, unique basement membrane constituents, and/or labeling perfused microvessels via the intravascular injection of a dye or fluorescently tagged antibody to visualize blood flow through microvessel lumens.[40-42] All of these labeling methods provide a means of contrasting microvascular architectures with the surrounding tissue when paired with a suitable imaging modality. The particular choice of vascular marker and imaging method should be carefully evaluated based on the biological questions being examined and determined based on requirements for resolution, signal to noise, tissue penetration depth, imaging location in terms of in vivo/ex vivo, and labeled cell specificity.[38] The relative importance of the various labeling and imaging considerations for microvascular visualization depends on the nature of the research and biological questions asked. For example, with investigations focusing on angiogenesis and subsets of vessel types, cell labeling of specific subpopulations is essential, while for studies characterizing blood flow, accurate vessel diameter and connectivity between vessel segments have greater significance. Moreover, effective pairing of these technologies with a particular imaging approach requires an understanding of the fundamental strengths and weaknesses of the options available.

2.1 | Markers of microvasculature

A critically important aspect of studying blood vessels is carefully tailoring biological interpretations and conclusions to appropriately correspond to the specific cell types or structures visualized (Table 1). An example that illustrates incongruity between data and interpretation is when vessels are labeled via

Condition	Mortality	Roles of Microvasculature		
1 Heart Disease	24%	Impaired Angiogenesis	Pulmonary Hypertension	Tissue Hypoxia
2 Cancer	22%	Pathologic Angiogenesis	Capillary Hyperpermeability	Metastasis Route
3 Lower Respiratory Diseases	5.7%	Capillary Dropout	Tissue Hypoxia	Capillary Hyperpermeability
4 Stroke	5.4%	Tissue Hypoxia	Capillary Constriction	Capillary Flow Dropout
5 Accidents Injuries	5.2%	Angiogenesis	Clot formation	Immune Cell Recruitment
6 Alzheimer's Disease	4.1%	Attenuated Vasodilation	Amyloid Angiopathy	Tissue Hypoxia
7 Diabetes Mellitus	2.9%	Capillary Hyperpermeability	Pericyte Loss	Capillary Dropout
8 Pneumonia & Influenza	2.1%	Impaired Oxygen Absorption	Immune Cell Recruitment	Capillary Hyperpermeability

FIGURE 1 The significance of the microvasculature in top causes of death and disease in United States. Top eight classes of fatal disease or injury with the fraction of annual deaths in the United States. Included with each malady are three highlighted fundamental roles the microvasculature plays with initiation, maintenance, or treatment (see main text for references)

perfusion of fluorescent dye[43] and general conclusions are made about vascular remodeling, disregarding changes in structure of nonperfused vessels, vessel neosprouts, and regressing vessels.[44] Even with specifically worded conclusions, focusing on findings that only quantify portions of the microvascular architecture represents an incomplete analysis and may omit significant remodeling events. Another key example is the use of superfused IB4 lectin, a marker commonly used to label blood vessels that also labels pericyte[45] and macrophages[46] (Figure 2A). Especially in development, many papers prematurely conclude changes occur in vascular architecture based on lectin staining[47,48] while omitting the issue that a mix of cell types are labeled, especially with the inability to differentiate structures between pericyte and endothelial cells. Studies that use Col-IV staining to quantify microvascular architecture[49] have similar shortcomings, labeling not just blood vessels[50] (Figure 2B), but other cell types such as pericytes and fibroblasts.[51] Additionally, Col-IV also marks thin bridges between capillaries previously referred to as Col-IV sleeves,[52] string vessels,[53] and acellular capillaries[54] in various tissues such as retina,[54] brain,[55] and muscle. Especially in the retina, this feature

TABLE 1 Markers of the Microvasculature

Diagram					
Name	Type	endothelial cells	pericytes	smooth muscle cells	Other
PECAM/ CD31	Surface[136]	✓[137]	✗[138]	✗[139]	Platelets, T-cells. leukocytes[137]
IB4 Lectin	Var.[140,141]	✓[46,142]	✓[45]	✓[143]	Macrophages[144], microglia[46], monocytes[145]
Col-IV	ECM[40]	✓[146]	✓[147]	✓[148]	Fibroblasts[149], MSCs[150]
Laminin	ECM[151]	✓[152]	✓[152]	✓[152]	Fibroblasts[153], epithelial cells[154]
CD34	Surface[136]	✓[155]	✗[156]	✗[157]	MSCs, HSCs, muscle satellite cells, fibrocytes[158]
VE-cadherin	Surface[138]	✓[138]	✗[159]	✗[160]	None[161]
EMCN	Surface[162]	✓[163]	✗[164]	✗[164]	Putative hematopoietic progenitor cells[165]
vWf	Internal[166]	✓[167]	✗[167]	✗[168]	Megakaryocytes[166]
aSMA	Internal[169]	✗[169]	✓[170]	✓[171]	Fibroblasts[172], perisinusoidal cells[169]
MYH11	Internal[173]	✗[173]	✓[174]	✓[175]	None[174]
NG2	Surface[176]	✗[176]	✓[157]	✓[156]	Microglia[170], macrophages, oligodendrocyte porogenitors[177]
N-Cadherin	Surface[178]	✓[179]	✓[159]	✓[180]	MSCs[181], fibroblasts[159], osteoblasts[159]
Desmin	Internal[182]	✗[168]	✓[183]	✓[156]	Interstitial cells, muscle satellite cells[158]
PDGFRβ	Surface[184]	✗[185]	✓[156]	✓[156]	MSCs[156], fibroblasts[156], some neurons[156]
Perf. PECAM	Surface[186,187]	Perf.[186]	✗[138]	✗[138]	Platelets[188], leukocytes[158]
Perf. Neuro-Trace	Internal[189]	✗[189]	Capillary[186]	✗[189]	Other neuronal cells when *fixed* (brain)[189]
FITC	Passive[42]	Perf.[42]	✗[42]	✗[42]	None[42]
Tie2	Surface[190]	✓[64]	✓*[64]	✓*[64]	Monocytes, macrophages[67], HSCs[191]
Dextran	Passive[192]	Perf.[192]	✗[192]	✗[192]	None[193]
VEGFR2, FLK-1	Surface[194]	✓[194]	✗[139]	✗[139]	HSCs[195], macrophages[196], neurons[197]
VEGFR1, FLT-1	Surface[198]	✓[198]	✗[199]	✗[199]	HSCs, macrophages[196], neurons[197]

EC, endothelial cell, ECM, extracellular matrix; HSC, hematopoietic stem cell, MSC, mesenchymal stem cell, Perf., perfused; PC, pericyte, SMC, smooth muscle cell; Var., various. **Labeling**: yes (✓), no (✗).

Note: Table shows general trends, there are exceptions with specific tissues, species, and disease conditions. *See main text.

is interpreted as a sign of collapsed or regressed vessels, yet this has never actually been established. There is a clear separation between the two structures in thickness (Figure 2C) and with the cross-sectional pixel intensity profile between lumenized vessels and Col-IV tracks (Figure 2D), with a lack of structures found in an intermediate or transitioning phenotype. An alternative hypothesis would be pericytes extending off-vessel processes[56] and secreting Col-IV.[57] For instances where the cell type responsible for an immunostained structure is not established with confidence, we caution interpreting results are cell-type specific, even if previously stated in the literature.

Another challenge for marking the microvasculature is identifying effective markers for PCs. Pericytes have no well-established cross tissue exclusive marker, making them hard to target for analysis,[58] although recent system-level analyses have revealed novel candidate markers that await confirmation.[59] A major point of contention with pericytes markers includes consensus with ASMA expression in pericytes, which is thought to be absent in pericytes on capillaries throughout some tissues, such as retina.[60] However, recent evidence indicates that this may be a product of how tissue samples are processed: In the retina, it was shown that if standard fixation techniques are used with ASMA staining, capillary pericytes
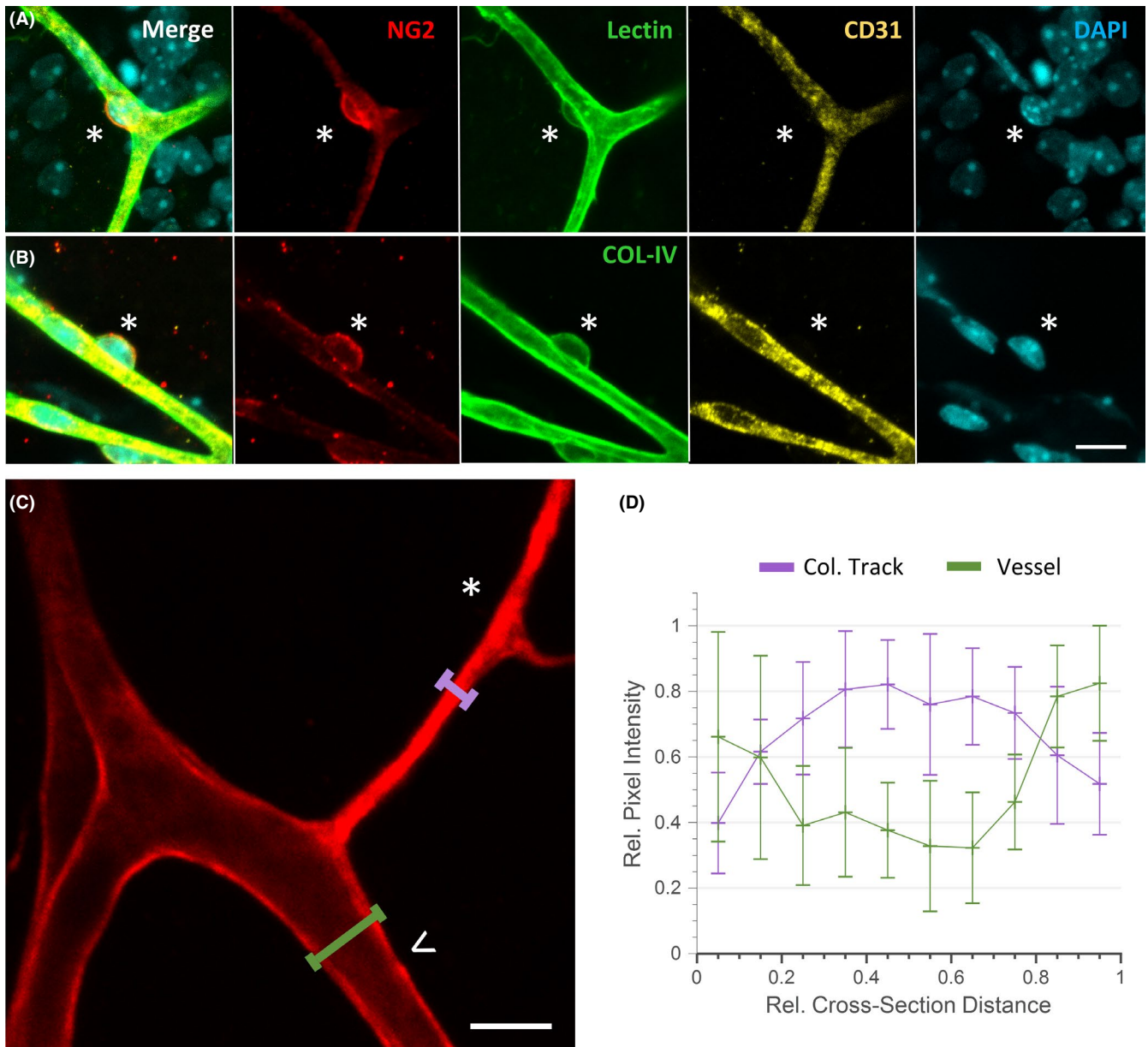
FIGURE 2 Both endothelial cells and pericytes share markers used in the literature for labeling endothelial cells, and Col-IV tracks, assumed to be regressed vessels, lack a pixel intensity profile indicative of a lumen. (A) Retina capillary with pericyte (NG2, red), IB4 lectin (green), endothelial cells (CD31, yellow), and cell nuclei (DAPI, cyan). (B) Retina capillary with pericyte and endothelial cells labeled with Col-IV (green; scale bar 10 μm). (C) High-resolution image of Col-IV off-vessel track (star) and lumenized blood vessel (arrow; scale bar 5 μm). (D) Comparison of Col-IV relative pixel intensity profile across cross-section of blood vessels and collagen tracks (P = 8.11E-6, 2-way analysis of variance, N = 10 vessels and tracks, error bars are standard deviation)

Name	Species	Sub Pop.	Cell Type Overlap
Tie2-GFP	Ms, Zb[200]	EC[200]	None[201]
Tie2-Cre-GFP	Ms	EC[202]	HSCs[203]
Tie2-CreERT2-EGFP	Ms	EC[204]	None[205]
VE-Cad-Cre-GFP	Ms	EC[206]	Lymphatic endothelial cells[206]
VE-Cad-CreERT-GFP	Ms	EC[207]	None[208]
FLT1:GFP	Ms[209], Zb[210]	EC[210]	Migratory angioblasts[210]
FLK1:GFP, RFP	Ms[211], Zb[212]	EC[213]	None[212]
My11-CreERT-YFP	Ms	PC, SMC[174]	None[175]
PDGFRB-CreERT2-TOM	Ms	PC,SMC[214]	Glial cells[214]
NG2-Dsred	Ms	PC, SMC[156]	Oligodendrocyte progenitors[215]
NG2-Cre-ERT2M	Ms	PC, SMC[216]	Oligodendrocyte precursors[205]
Tie1-EGFP	Ms	Embryonic EC[217]	None[217]
PDGFb-CreERT2	Ms	ECs[218]	None[218]
β-Actin-GFP	Ms	EC, PC[219]	Not examined[205]
α-SMA-GFP, RFP[220]	Ms	Sub. PC, SMC[221]	None[221]
α-SMA-CreERT2	Ms	Sub. PC, SMC[222]	None[222]

EC, endothelial cell; HSC, hematopoietic stem cell; PC, pericyte; SMC, smooth muscle cell. **Species**: Ms, mouse; Zb, zebrafish.

Note: Labeling can vary across tissues, and in most cases not rigorously verified.

are ASMA-negative,[61] but if the samples were snap frozen with methanol fixation to prevent actin depolymerization, at least half of capillary pericytes are ASMA-positive.[61] We suspect that major portions of other canonically known ASMA-negative pericyte populations across tissues might actually express this marker, and there is a possibility that ASMA is, in fact, a pan marker for pericytes that requires a more sensitive measurement technique to confirm. However, even if ASMA is expressed by all pericytes to some degree, it is not a unique marker for pericytes, because it is also expressed by vascular smooth muscle cells.

Finally, the expression of Tie2 by pericytes has been fiercely debated in the past decades, with extensive characterization of Tie2 expression in cultured pericytes,[62] but a lack of Tie2 expression noted in pericytes in vivo.[63] However, recent evidence has shown that a pericytes-specific knockout of Tie2 leads to dramatically altered vascular structure, paired with a demonstration of Tie2 acting as a potent pericyte chemokine in vitro,[64] together suggesting that Tie2 signaling may serve an important role in pericyte function. However, this finding awaits confirmation with the development of effective antibodies or other methods to directly label Tie2 in tissue and demonstrate pericyte expression in vivo. This controversy highlights the need to utilize measurement techniques that avoid such complications with variable results from tissue processing, such as fluorescent in-situ hybridization[65] which measures RNA expression of the target gene directly.

2.2 | Animal models with endogenously labeled vasculature

An increasing number of transgenic murine models have been developed to visualize the microvasculature, including those that contain cell-type specific fluorescent reporters for endothelial cells, smooth muscle cell, and pericytes (Table 2). We emphasize there is an important limitation of these reporter models that is often ignored: these animal models often only include the proximal endogenous reporter region with the fluorescent reporter, meaning that gene expression behavior from distal enhancers is often lost. An example of this is with Tie2 expression, which has been found in other cell types such as HSCs.[66] and neutrophils, endothelial progenitor cells, macrophages,[67] pericytes, [62] and keratinocytes.[68] Yet the primary Tie2-GFP mouse model is only known for GFP expression exclusively in endothelial cells,[69] in this case serving as an advantage with a reporter line that appears to selectively label the vasculature and not track other cell types known to have endogenous expression.

2.3 | In vitro and ex vivo models to study the microvasculature

Over the last century, various models have been used to study the complexity of the microvasculature, including those that utilize

cultures of various cell populations, tissue explants, and animal models (Table 3). Historically, researchers have had to consider significant trade-offs when choosing between different model systems. In vivo models typically have the best chance of recapitulating human disease since pathologies are heavily influenced by the complex interplay of a multitude of cell types.[70] However, this benefit comes at a cost: In vivo models are usually limited by throughput, exhibit high cost in time and resources, and imaging techniques restricted by limitations with sedation duration, subject restraint, and detector scan speed. Furthermore, typically any intervention short of a cell-specific knockout of an implicated gene will not establish cellular mechanism, which can take years to generate in an in vivo model. In vitro models typically exhibit much higher throughput and have a wider range of available analysis tools to characterize the system,[71] but at the cost of greater simplification and abstraction of tissue structure and disease conditions compared to in vivo, such as lacking various cell types or blood flow.

However, the trade-offs between in vivo and in vitro models are blurring now more than ever. Advances in new imaging techniques allow for in vivo imaging that provides the opportunity for higher throughput and fully temporal measurements in various tissues. The latest in vivo gene editing techniques, such as CRISPR/Cas9,[72] have made targeted genetic alterations easier, yet there are still challenges remaining with regards to efficiency and off-target binding of genetic payloads.[73] At the same time, advances in 3D bioprinting, biomaterial

TABLE 3 Model Systems of Microvascular Architectures

Name/ Tissue	Type	Species	Throughput	Noninvasive Setup	Δ Vaso. Diameter	Timelapse	Adult	Angiogenesis	Network	Lumen	Flow	Mural
Chick Chorioallantoic Membrane	In vivo	Ch[223]	++	✗	✓	✓	✗	✓	✓	✓	✓	✓
Mesentery	In vivo	Ms[224], Rt[225], Ct[226]	+	✗	✓	✓	✓	✓	✓	✓	✓	✓
Gluteus Maximus	In vivo	Ms[227]	+	✗	✓	✓	✓	✓	✓	✓	✓	✓
Vessel Segments from Resistance Arteries	Ex vivo	Ms[228], Hm[229]	+	✗	✓	✓	✓	✗	✓	✓	✗	✓
Skeletal Muscle	Ex vivo	Ms[230], Rt[231]	+	✗	✓	✓	✓	✓	✓	✓	✓	✓
Cremaster	In vivo	Ms[232], Rt[233]	+	✓	✓	✓	✓	✓	✓	✓	✓	✓
Retina	Ex vivo	Ms	+	✓	✗	✗	✓	✓	✓	✓	✓	✓
Embryoid Explant	In vivo	Zb[234], Ms[235], Fg[236]	++	✗	✓	✓	✗	✓	✓	✓	✓	✓
Cornea Limbal	In vivo	Ms[237]	+	✓	✓	✓	✓	✓	✓	✓	✓	✓
Microfluidic EC Chip	In vitro	Var[238]	+++	✗	✗	✓	~	✓	✓	✓	✓	✗
EC-PC Matrix Co-culture	In vitro	Var[239,240]	++++	✗	✗	✓	~	✗	✓	✓	✗	✓
EC-PC Transwell	In vitro	Var.[239]	++++	✗	✗	✓	~	✗	✗	✗	✓	✓
EC Culture	In vitro	Var.[239]	++++	✗	✗	✓	~	✓	✓	✓	✓	✗
Dermal	In vivo	Ms[44]	+	✓	✓	✓	✓	✓	✓	✓	✓	✓
Developing Retina	In vivo	Ms.[241]	+	✗	✓	✗	✗	✓	✓	✓	✓	✓
Embryoid Body	In vivo	Ms.[242]	+++	✗	✗	✓	✗	✓	✗	✗	✗	✓
Brain Explant	Ex vivo	Ms.[243]	++	✗	✓	✓	✓	✓	✓	✓	✗	✓
Retina Explant	Ex vivo	Ms.[244,245], Rt.[246]	++	✗	✓	✓	✓	✓	✓	✓	✗	✓
Allantois Explant	Ex vivo	Ms.[247]	++	✗	✓	✓	✗	✓	✓	✓	✗	✓
EC Microbeads in Fibrin	In vitro	Var.[248]	++++	✗	✗	✓	~	✓	✓	✓	✗	✗

EC, endothelial cell; PC, pericyte. **Species**: Ch, chicken; Ct, cat; Fg, frog; Hm, hamster; Ms, mouse; Rt, rat; Var., various; Zb, zebrafish. **Features**: yes (✓), no (✗), various (~). **Throughput**: measure of degree of throughput for each protocol. **Noninvasive setup**: if model setup requires an invasive procedure. **Δ Vaso. Diameter**: if vasoconstriction or vasodilation can practically be examined in a real-time fashion. **Timelapse**: if system can practically be imaged continuously in a real-time fashion. **Adult**: if tissue analyzed is from adult or embryonic. **Angiogenesis**: if angiogenesis can be observed. **Network**: if model either has existing vascular network or can form a network. **Lumen**: whether vascular structures have a lumen. **Flow**: if vascular structures exhibit flow in model system. **Mural**: if smooth muscle cells and pericytes are included.
Note: Table is meant to capture general trends for what is feasible in a standard version of the experiment setup, there are exceptions.

TABLE 4 Imaging Modalities for Vascular Networks

| Name | Resolution | | Z Depth | Flow | Oxygen | Mechanism | Trade-offs |
	Z	XY					
Bright field	1 µm[249]	0.25 µm[249]	50 µm[38]	✗	✗	Absorbance[250]	+ Visualize outlines of cells[250], low cost + Temporal resolution − Excites fluorophores outside of imaging area[250] − Image is blurred by emission from out-of-focus regions[250]
Fluorescent Widefield	1 µm[251]	0.25 µm[251]	50 µm[38]	✗	✗	Fluorescence[250]	+ Temporal resolution: milliseconds[252], low cost − High resolution requires immersion objectives[251] − Image is blurred by emission from out-of-focus regions[250]
Point Scanning Confocal	0.50 µm[251]	0.18 µm[251]	100 µm[253]	✗	✗	Fluorescence[252]	+ Pin-hole reduce out-of-focus light[250] + Temporal resolution: milliseconds[252] − Phototoxicity, photobleaching[254]
Spinning Disk Confocal	0.75 µm[254]	0.25 nm[254]	100 µm[38]	✗	✗	Fluorescence[252]	+ Higher FPS compared to point scan[250] + Less phototoxic to cell, less photobleaching[250] − Poorer filtering of out-of-focus light compared to point scan[250] − Lower resolution, smaller FOV[254]
Two Photon	0.4 µm[251]	0.20 µm[251]	1 mm[255]	✗	✗	Fluorescent[256]	+ Useful for thick specimens (>200um)[250] + Bleaching limited to imaging plane[251], low light scatter[256] + NIR light less phototoxic than VIS − Enhanced heating from NIR light − Broader excitation, pronounced photobleaching[257]
Photo-acoustic	1 µm[258]	10 µm[258]	5 mm[259]	✓	✓	Flow, oxygenation[260]	+ High contrast and spatial resolution, high framerate[260] + Imaging thick tissues (>1 cm)[260] − Increased resolution at expense of ultrasonic penetration[260] − Comparably low resolution[260]
Laser Doppler		1 µm[261]	1 mm[261]	✓	✗	Flow[262]	+ Live imaging of flow[262] − Long mapping time[262]
Laser Speckle		10 µm[263]	1 mm[264]	✓	✗	Fluorescence[265]	+ Resolution adequate for low-flow microvasculature[265] + Noninvasive, live imaging[265], real-time changes in flow[265] − Requires knowledge of blood velocity distribution[262] − Motion artifacts[265]
Second Harmonic	2.5 µm[266]	0.70 µm[266]	300 µm[267]	✗	✗	Auto-fluorescence[268]	+ Three-dimensional resolution[269], NIR wavelength + Label free[267], Long imaging times[269] − Low image quality in deep tissue[270]
Optical Coherence Tomography	2 µm[271]	1 µm[271,272]	2 mm[253]	✓	✗	Reflectance[273]	+ Temporal resolution: seconds[252], label free[274] + Technology contained in endoscopes, handheld probes[271] − Angiography visualizes only flow, not leakage[274]
RESOLFT, STED	50 nm[250]	30 nm[275]	300 µm[276]	✗	✗	Fluorescence[252]	+ Video-rate, live-cell imaging[252] + Temporal resolution: seconds[252] − Requires highly-stable fluorophores[252]
FPALM	50 nm[250]	20 nm[275]		✗	✗	Fluorescence[252]	+ Fast framerate for high resolution[252], live-cell imaging[252] + Image single molecules/single particle tracking[252] − Requires photo-switchable fluorophores[252]
Electron Microscopy	8 nm[277]	1 nm[252]	<1 µm[278]	✗	✗	Fluorescence[252]	+ High resolution[252] − Limited labeling options[19], no temporal resolution[252,279] − Restrictive sample prep.[252,279]
Light-Sheet	0.75 µm[280]	0.25 µm[280]	10 mm[264]	✗	✗	Fluorescence[280]	+ Excellent optical sectioning 3D imaging[281] + Low bleaching and phototocicity[281] − Restrictive sample prep[281]

research, and patient-specific primary cell culture allow for more advanced in vitro models, although there is still difficulty with cell collection in these systems for subsequent analysis.[71] Indeed, the number of available model systems has been growing, and with the advent of new analysis techniques, the opportunities to collect data from microvascular network architecture have increased dramatically and reveal new prospects for efficient and reproducible data capture.

3 | STATE-OF THE-ART IMAGING MODALITIES FOR MICROVASCULAR NETWORKS

There are a vast range of techniques available for imaging the microvasculature, with trade-offs between resolution, signal penetration, and acquiring multiplexed functional readouts, such as

(A) Vessel Area Fraction

Blood vessel area divided by **total image area**

Spatial vessel density that incorporates vessel thickness.
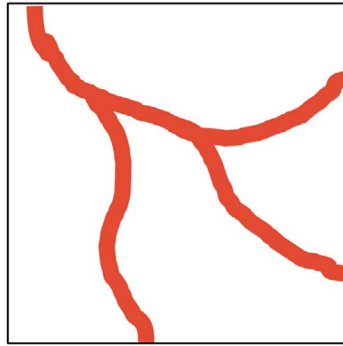
(B) Vessel Length Density

Length of **blood vessel centerline** divided by **total image area.**

Spatial vessel density, oxygenation/nutrient delivery dysfunction
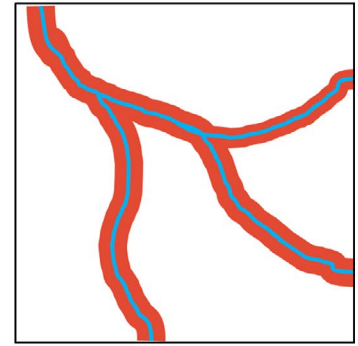
(C) Vessel Diameter

Distance between edges orthogonal to **centerline** of **blood vessel.**

Radial thickness of vessels, revealing instance of dilation, sprouting, vessel regression
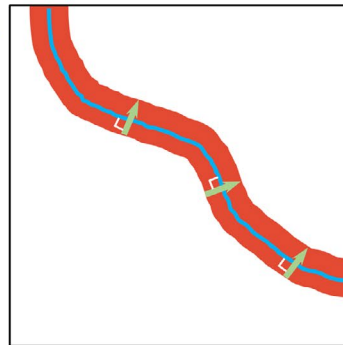
(D) Branchpoint Density

Count of **branchpoints** divided by **vessel centerline** length or total **image area.**

How interconnected the vessel network is, indicating resistance to occlusion or blockage, flow dynamics
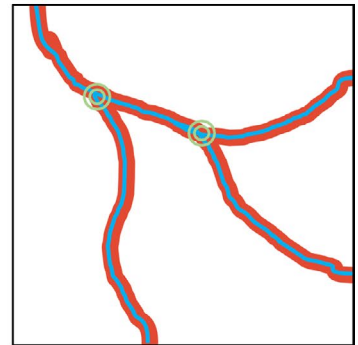
(E) Tortuosity

Segment length divided by **endpoint distance** Integral between **Segment line** and **line between endpoint**

Vessel remodeling, activation
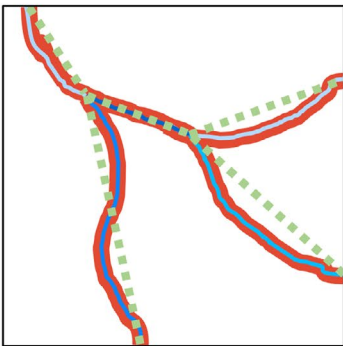
(F) Lacunarity, Fractal Dimension

Identifies **repeating structures** of **blood vessel** across range of scales of vasculature viewed as fractal.

Self similarity of vascular structure across scales.
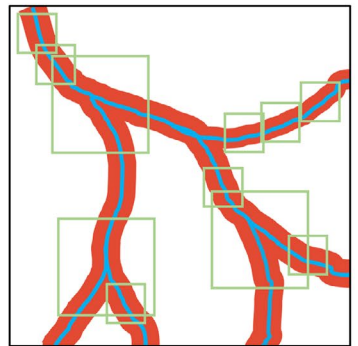
(G) Extra-vascular Diffusion Distance

Max distance from **vessel** for each hole.

Measure of degree or heterogeneity of tissue oxygenation.
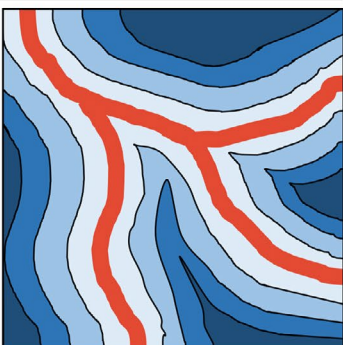
(H) Vessel Segment Partitioning

Count of **segments** divided by **vessel segment centerline length.**

How interconnected the vessel network is, indicating resistance to occlusion or blockage, flow dynamics.
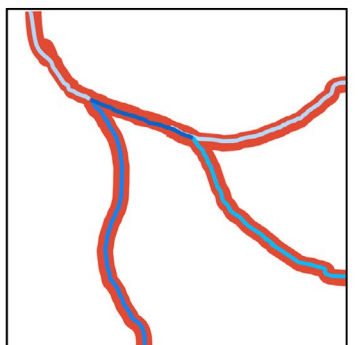
FIGURE 3 Basic metrics quantifying the complexities of the microvascular architecture. Visual explanation of metrics that have been used to quantify various aspects of microvessel network architecture, including (A) VAF, (B) vessel length density, (C) vessel diameter, (D) branchpoints density, (E) tortuosity, (F) lacranuity and fractal dimension, (G) extra-vascular diffusion distance, and (H) vessel segment partitioning

Heart
(A)

Diaphragm
(B)

Skeletal Muscle
(C)

Liver
(D)

Peritoneal Cavity
(E)

Inguinal Fat
(F)

Retina

Superficial Plexus
(G)

Intermediate Plexus
(H)

Deep Plexus
(I)
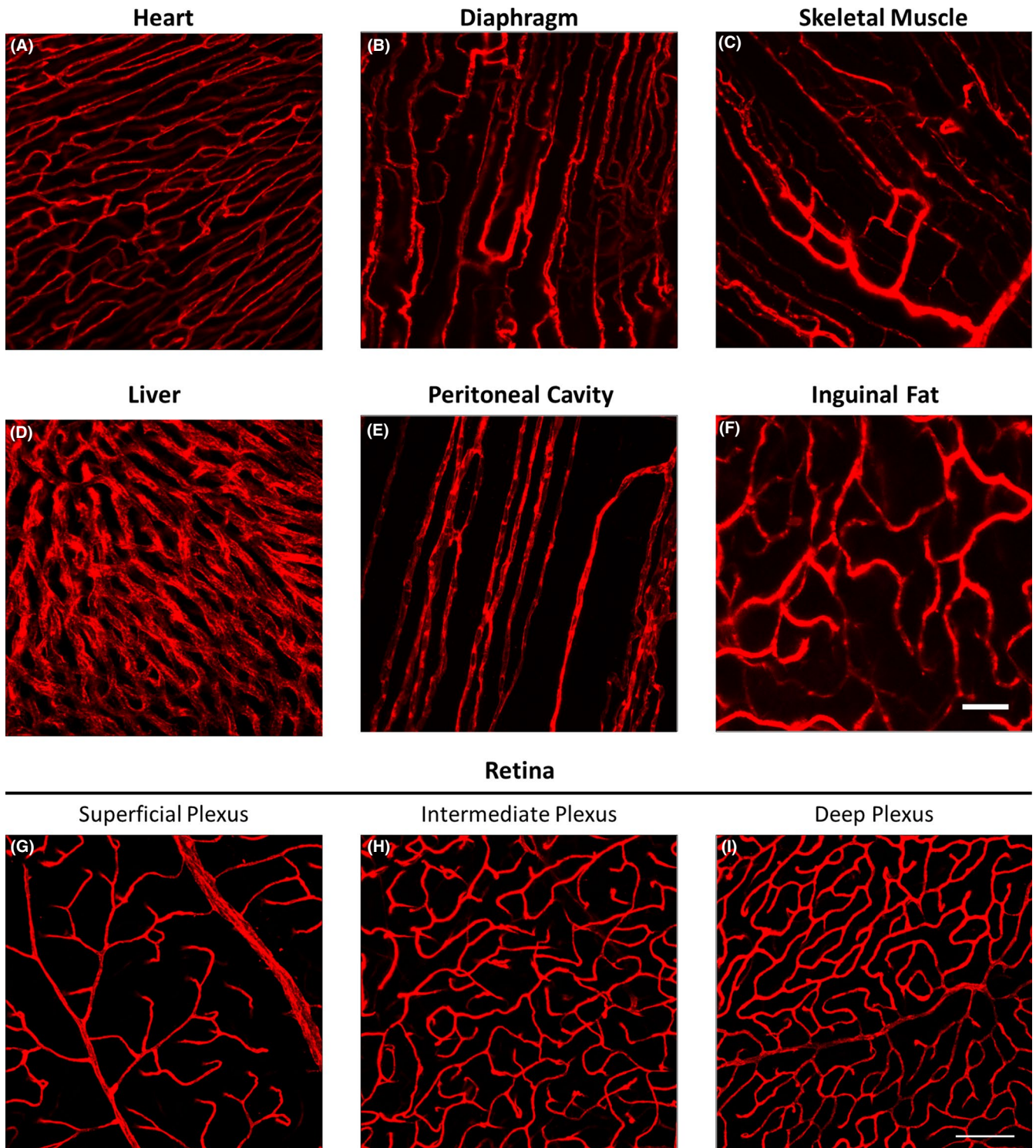
FIGURE 4 Heterogeneity of blood vessel network structure across and within tissue. IB4 lectin Perfused microvessels of (A) heart, (B) diaphragm, (C) skeletal muscle, (D) liver, (E) peritoneal cavity, (F) inguinal fat, and of the three distinct vascular layers of the retina (G-I; scale bar 50 μm)

blood flow and tissue oxygenation (Table 4). Beyond the classical fluorescent-based imaging modalities that have been a mainstay for imaging microvascular structure, there now exist several new technologies that also quantify microvascular function. Advances in photoacoustic microscopy have recently enabled imaging of a wide range of tissue depots, larger fields of view, and higher resolutions, along with capturing other functional data such as blood flow velocity and tissue oxygenation.[74] The technology behind OCT, an imaging technique based on reflected light and measuring time of flight for photons, has recently improved with resolution to the point where these imaging modalities can successfully image the microvasculature.[75] New super resolution imaging techniques
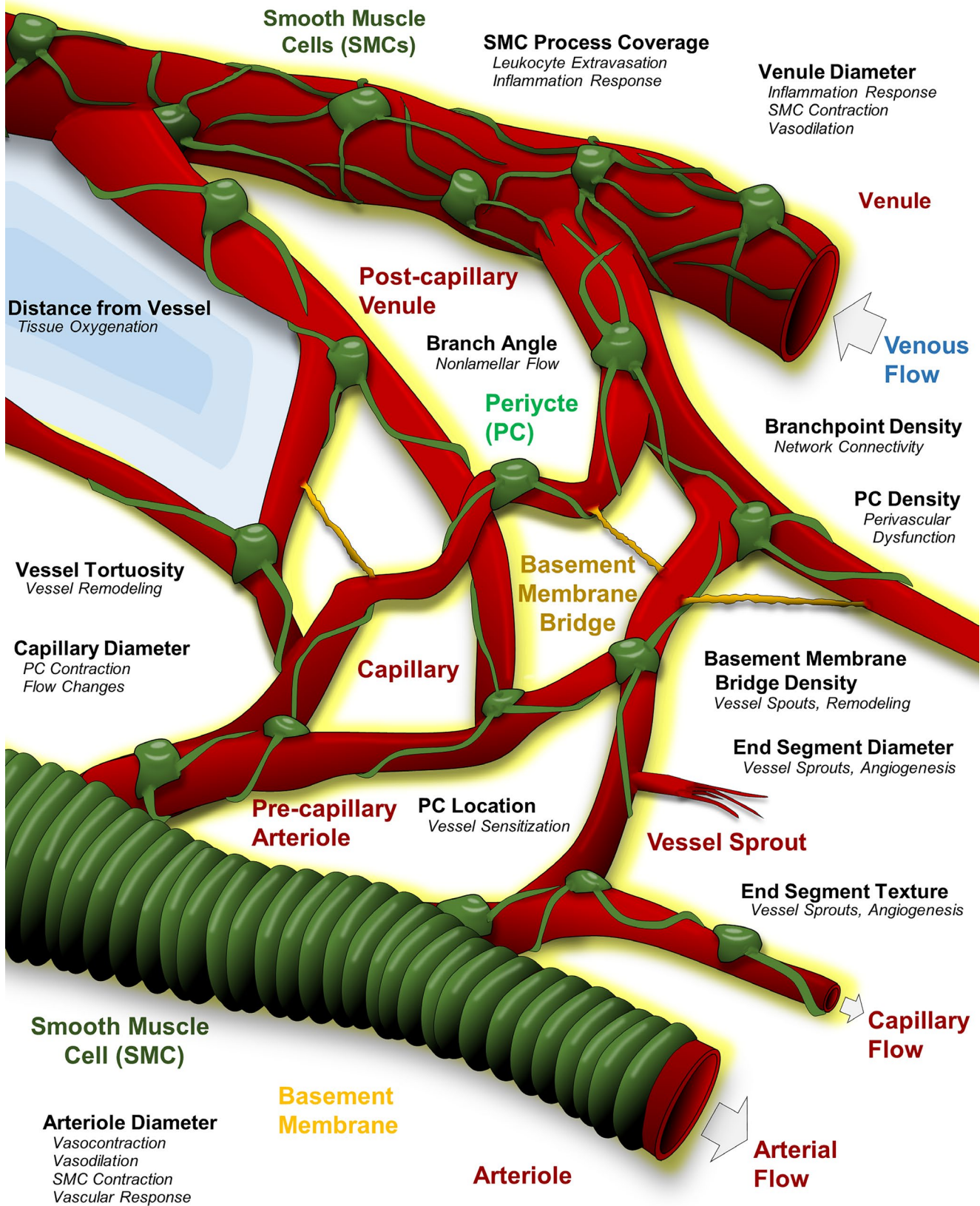
FIGURE 5 Bridging form and function: correspondence between microvasculature architecture metrics and biological behaviors. Schematized microvasculature network with various cellular and acellular components (multicolored font) mapped to quantitative image analysis metrics that indicate different aspects of microvascular function (black font)

TABLE 5 Vessel Network Analysis Tools

Name	Lang.	Application	Metrics	Validation	Cts	Yr	Cts/yr
AngioQuant[83]	MATLAB	Brightfield, Cell Culture	Segment Count, VL, VA, VAF, Segment Area, BP, BP/Segment Count	QT BD	104	2005	8
RAVE[81]	MATLAB	Fluorescent, Tissue	VAF, VLD, VR, FD	QT manually analyzed BD for VAF, VLD, and VR. Basic *In silico* for FD	24	2011	3.4
Vessel Analysis ImageJ Macro	ImageJ Macro	Brightfield, Tissue	VAF, VLD	None	-	-	-
AngioTool[78]	Java, ImageJ	Fluorescent, Tissue	VAF, SC, VL, VLD, EP, lacunarity, BP/area	QL manually analyzed BD	111	2011	15.9
CSAQ[282]	*Web Based*	Brightfield, Tissue	VL, VAF, BP; Contrast, Entropy	Manual (BP), QT comparison to AngioQuant	24	2008	2.4
Breast Tumor Microvasculature Reconstruction[82]	MATLAB, JAVA	Micro Ct, Tumor	VLD, VD, SL, MEVDD, FD, Tortuosity, Flow	Metrics from BD within literature values	17	2013	3.4
VESGEN 2D[283]	Java, ImageJ	Brightfield/Flourescence, Tissue	VD, VT, FD, VAF, VLD, BP	QT BD	29	2009	3.2

BD, biological data; BP, branchpoints; EP, endpoints; FD, fractal dimension; MEVDD, max extra-vascular diffusion distance; NS, not specified; QL, qualitative; QT, quantitative; SC, segment count; SL, segment length; VLD, vessel length density; VD, vessel diameter; VR, vessel radius.

developed in the last decade, such FPALM and stochastic optical reconstruction microscopy, have allowed visualization of structures in details beyond the resolution limit of visible light, allowing for direct imaging of individual proteins and flourophores.[76]

4 | MICROVASCULAR NETWORK ANALYSIS AND QUANTIFICATION

The microvascular network forms a sprawling architecture of interconnected vessels that vascularize nearly all tissues in the body. Such complex spatial networks undergo remodeling in adult tissue as well as embryonic; in quiescence as well as pathologic. Understanding changes in vessel morphology cannot be captured by a single metric to quantify its structure: A range of metrics must be used to summarize various unique characteristics of the network. While previous work has developed a multitude of metrics for quantifying microvascular architecture, we believe that further work must be done in both developing new metrics and demonstrating that a given set of available metrics provide unique and useful information to answer biological questions. To this end, a series of suggestions are proposed to increase scientific rigor and reproducibility of quantifying the complexities of the microvasculature.

4.1 | Metrics for quantifying microvascular networks

Previous research has developed various metrics for microvascular network analysis (Figure 3A-G), including the fraction of image area

composed of blood vessels (VAF),[77] blood vessel length normalized by image field of view (vessel length density),[78] average vessel diameter of all vessels or divided by vessel type,[79] density of branchpoints,[80] tortuosity,[81] lacranuity,[78] fractal dimension,[81] and max extra-vascular diffusion distance to examine tissue oxygen perfusion.[82] Other metrics have been developed outside of this set but not standardized and adopted by consensus. Studies often normalize metrics in different ways, such as measuring branchpoints per image, normalizing to field of view, or normalizing to vessel length. We posit that metrics should be designed to encourage valid comparisons across research studies and should be normalized to facilitate this process. Thus, using a simple metric of vessel length[83] is not as useful as vessel length density, a metric that can be directly compared over a range of spatial resolutions and imaging modalities.

4.2 | Architectural features of microvasculature: bridging form and function

Capillary architecture possesses markedly different structures to meet the unique metabolic demands of peripheral tissues,[84] including the radial spoke-wheel structure of the retina, parallel beds of skeletal muscle, or dense networks of the liver (Figure 4A-F). Even within a single tissue such as the retina, there is impressive heterogeneity in microvascular architecture between tissue locations (Figure 4G-I). This tissue environment heterogeneity is further reflected by unique endothelial transcriptomes found in each organ[85] and distinct endothelial marker profiles at different parts of the vascular tree.[86]

With much of biology, function and form are closely intertwined[87]: the microvasculature is no exception. A wide range of

TABLE 6 Computation Models of Microvascular Architecture

Description	Language	Method	Type	Validation
Particle-based EC Network[284]	C++	ABM, CPM	Vasculogenesis	QT to classic CPM
Retina ABM[285]	NetLogo	ABM	Retinal developing vasculature	QT comparison retinal BD
3D CPM of Tumor Growth[286]	CompuCell3D	ABM, CPM	Tumor angiogenesis	QL to Macklin et al.[287]
ABM for Disruption of Vasculogenesis[288]	CompuCell3D	ABM	Vasculogenesis	QT to BD with AngioTool[78]
3D Sprouting Angiogensis[289]	NS	ABM	Sprouting angiogenesis	QT metrics within BD range
Hypoxic Vessel Sprouting[290]	NS	ABM Hybrid	Any 2D or 3D vessel formation in a tissue	QT comparison with BD
Tumor Angiogenesis and Patterning[291]	NS	ABM Hybrid	Sprouting angiogenesis	QT metrics within BD range
Angiogenesis with Discrete Random Walks[292]	NS	ABM Hybrid	Tumor angiogenesis	QL assessment of simulation results
ABM of Tumor Angiogenesis and Regression[293]	NS	ABM Hybrid	Tumor angiogenesis and regression	QL to BD
3D Phase Field ABM of Vascular Networks[294]	NS	ABM Hybrid	3D Angiogenesis	QL to basic theoretical behavior
Adaptive Network with Flow[295]	C	Stochastic Hybrid model	Flow, oxygen transport, and adaptation of existing network	Thorough quantitative comparison to experimental results across all categories
Multiphase Tumor Angiogenesis Growth[296]	CAST3M	Continuum Discrete	Tumor growth	QT comparison with BD
Vessel Generator for Cell-colocalization (CIRCOAST)[135]	MATLAB	Structural Descriptive Model	Static adult microvascular network for basic model validation	QT metrics within BD range
Tumor Angiogenesis with Blood and Interstitial Flow[297]	NS	Hybrid	Tumor growth	QT metrics within BD range

ABM, Agent-based model; BD, biological data; CPM, cellular pots model; QL, qualitative; QT, quantitative; NS, not specified.

biological behaviors, including blood vessel growth, regression, dilation, constriction, stability, and permeability, can be mapped to quantitative metrics of microvascular structure and give insight into physiologic and pathological function of the microcirculation (Figure 5). Beyond the adaptations of microvessel networks to support unique tissue metabolic environments, morphological changes in vessel structure are hallmarks of key vascular remodeling events. Spatial distribution of capillary networks determines spatial heterogeneity of oxygenation and nutrient delivery.[88,89] Enriched build-up of extra-cellular matrix can indicate a fibrotic response[90] to inflammatory conditions. Increased blood vessel tortuosity can indicate signs of endothelial cell activation and pathological microvascular remodeling and/or ischemia-induced arterialization in collateral microvessels.[91]

Moreover, certain quantification metrics may carry unique significance depending on the location analyzed within the vascular tree. For instance, changes in vessel diameter in arterioles suggest changes in vascular smooth muscle cell vasoconstriction to modulate vascular resistance,[92] capillary diameter changes are indicative of changes to pericyte contraction and distribution of flow and oxygenation,[93] and venule dilation suggests changes to blood capacitance

(storage)[94] or remodeling in response to inflammation to facilitate leukocyte extravasation from circulation.[95]

4.3 | The need for pairing perivascular and microvascular analysis

Analyzing changes to the perivascular space can yield just as important insights as the vasculature itself given the close cross-talk between endothelial cells and smooth muscle cell and pericytes. For example, changes in pericyte density are known to play a key role in the pathogenesis of diabetes,[27] and changes in pericyte locations relative to branchpoints[96] have been associated with changes to stability and sensitization of the microvascular network. We emphasize the need to analyze perivascular behavior as well as microvascular remodeling to truly understand the structure and function of microvascular networks: A common limitation of many studies is to study one or the other in isolation. Most existing software for quantifying microvascular network architecture accomplishes this by evaluating the endothelial network structure. There is one software package that can analyze perivascular cell recruitment to the vasculature through overlap of the two structures.[97] While this metric may be
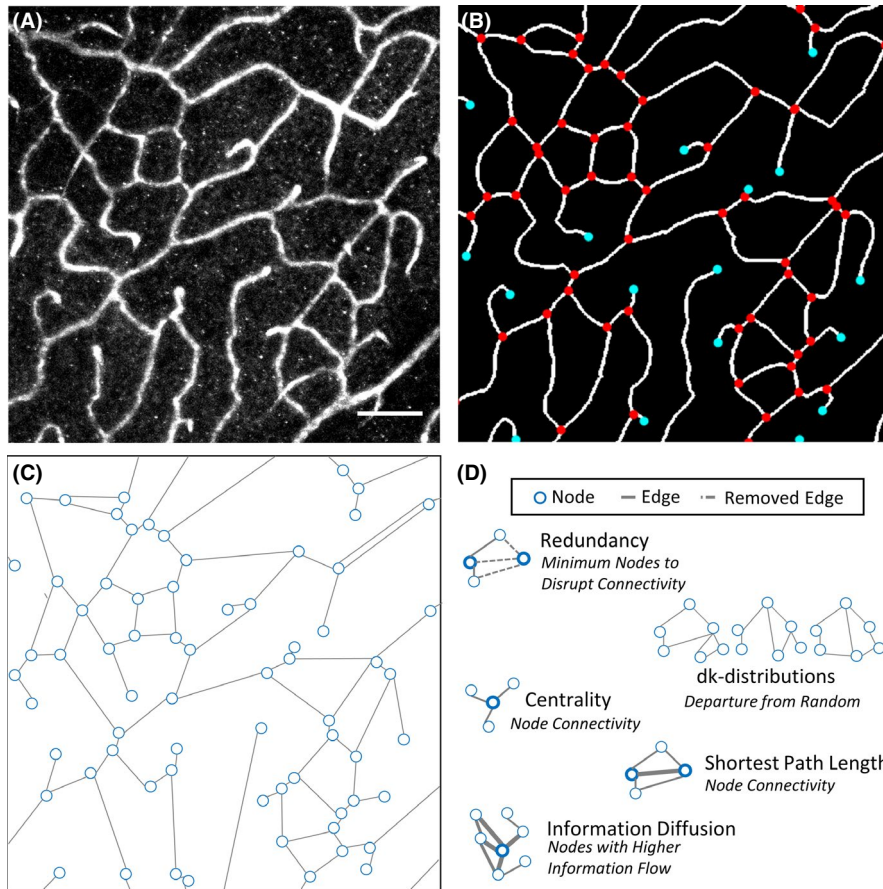
FIGURE 6 Novel image analysis metrics by analyzing the microvasculature with graph theory. A, Confocal microscopy image of the murine retinal deep vasculature, with CD105 marking ECs (white; scale bar = 50 μm). B, Image analyzed with basic segmentation, skeletonization, and branchpoints classification, with vessel centerline/skeleton (white), branchpoints (red), and EP (turquoise). C, Conversion of vasculature into a graph, with branchpoints indicated as "nodes" (blue) and vessel segments as "edges" (gray). D, Visual summary of types of metrics to quantify graphs, with removed edges representing change to network after a blood vessel has regressed or experiences obstructed flow

confounded by changes in perivascular or vascular density across study groups, and perivascular cells may associate with the vasculature with minimal channel overlap, this software allows researchers to begin to probe perivascular interactions with the microvasculature. A survey of the published literature reveals that the most common approach for analyzing perivascular cell coverage and/or morphology (eg, of pericytes,[98] smooth muscle cell,[99] or other cell types like macrophages[100] that are known to play key roles in angiogenesis and vessel remodeling[101]) is through manual or basic automated comparisons of thresholded area or nuecleii.[102] For example, basic cell counts can be obtained manually through ImageJ's cell[103] counting feature, the multipoint tool,[104] or using its particle analysis set of tools for automated analysis.[104] More extensive positional or morphological investigations of perivascular structures require custom image analysis solutions that have yet to be developed. Automated and quantitative analysis of microvascular networks paired with detailed analysis of smooth muscle and pericyte cell populations could become a standard pipeline that would enable better understanding of microvascular remodeling mechanisms and the development of new therapeutics for microvascular diseases.

4.4 | Software packages for quantifying microvascular networks

Alterations in microvessel network architecture have been used ubiquitously in studying vascular diseases, and there are a multitude of software packages available for quantifying changes in architecture (Table 5). Three, notably, have been used in a significant number of publications, namely AngioQuant, AngioTool, and RAVE.

AngioQuant has been developed to analyze endothelial networks in vitro, with a focus on quantifying various metrics of tubule formation using bright field images.[83] Recently, it has been adapted for use in evaluating higher resolution datasets of microvascular networks in vivo[105] and in histological samples.[106] Its validation is focused on quantification of in vitro experiments showing trends of changes with various metrics, but no statistical comparisons between study groups. The datasets were not validated against manually analyzed images and there is no analysis included comparing accuracy and overall performance between AngioQuant and other available software packages.

AngioTool is presented as a quick, hands-off, and reproducible image analysis tool, deployed as an ImageJ plugin, for quantification of microvascular networks in microscopic images.[78] The validation of AngioTool included analyzing biological data from murine hindbrain and retina using various metrics, including visualized vessel segmentation, vessel centerline, and branchpoints presented for qualitative inspection. For quantitative biological validation, endothelial cell explants were cultured and analyzed with two drug treatments that were known to alter vascular structure as a positive control.[78] Additionally, output metrics were validated with a subset of manually counted images in an unblinded fashion with two investigators.

RAVE is an image analysis tool that can be used on a wide array of images[81] to accelerate the unbiased, quantitative analysis of

microvasculature architecture. Validation for this tool included comparing automated outputs generated by RAVE to manual analysis of various morphometric parameters for in vivo microvessel networks in murine spinotrapezius muscle tissue and in a xenograph tumor model. A dataset of images was compared to manually processed images with a Bland-Altman analysis.

4.5 | Improving vessel quantification, analysis, and interpretation

We estimate that these software packages are largely underutilized, based on the high number of published manuscripts that refer to the quantification of microvessel architecture. Indeed, a search on PubMed on relevant terminology (terms used included: microvasculature density, capillary dropout, pericyte dropout; see all terms in Appendix S1) reveals over 120 000 publications to date. While this query includes publications that merely mention the terms searched for, the nearly three order-of-magnitude difference between citations of these software programs compared to this large collection of publications suggests that there is an unmet need for vessel architecture analysis beyond the available options, with researchers often resorting to manual ad hoc analysis of microvessel networks, leading to decreased repeatability, comparability, and scientific rigor. We propose the following design criteria for an effective software package:

- **Ground truth validation:** A rigorous and complete validation of software requires a comprehensive analysis of multiple types of datasets. This includes an extensive comparison of automated results to manually processed images, not just with output metrics, but also with the pixel-by-pixel raw segmentation, skeleton centerline, and branchpoints locations quantified with a combination of false positive rates, false negative rates, Bland-Altman analysis, and SSR. Ideally, this manual comparison would include multiple study groups with known vascular differences in architecture between them.
- **Biological validation:** Validating the automated pipeline with several biological datasets with known differences (biological positive controls), ideally from different tissue and/or imaging resolutions, will demonstrate the efficacy of the program in practice. This analysis demonstrates that the program can detect true positives in actual dataset, where a real change is detected between study groups.
- **In silico validation:** Program development needs to be paired with a validated parameterized computational model that can generate artificial in silico vascular networks[107] to verify that changing basic parameters of the model yields expected changes in metric output with the image analysis pipeline.
- **Quantitative comparisons between previously developed programs:** The field benefits far less from releasing another "one-off" vessel image analysis program independent from previous work and instead should test and demonstrate its efficacy compared to existing software. Outputs from each program and manual analysis should be compared, including output metrics, raw segmentation, skeletonization, and branchpoints assignment in the form of false positive and negative error rates, Bland-Altman analysis, and SSR. Execution time should also be critically evaluated and reported, given the importance of balancing throughput with accuracy.

- **Standardized metric sets:** Each software program has a unique collection of metrics that are often calculated using different methods. A consensus of metrics needs to be established in the interest of rigor and reproducible science. An example of this would be measuring branchpoints: Some packages display raw counts, while others normalize to image area or vessel length.
- **Effectiveness of metric collections:** Methods should be developed to not only test and validate each method but also demonstrate their usefulness as a collection in determining changes in the vascular architecture. Analysis needs to be done to show that these new metrics provide unique non-correlative information compared to existing metrics, utilizing techniques developed from the field of feature selection.[108]
- **Effect of image quality on output metrics:** An examination needs to be performed with respect to how the program performs when image quality varies between study groups from batch effects, or simply has a high degree of variance. Image quality of the datasets provided with these software packages often appears ideal. High variance with image quality may skew segmentation results and output metrics, so output metrics across a range of image qualities should be examined.
- **Effect of parameter adjustment:** Some software packages allow for adjustment of key image processing parameters to enhance results, but the effect (and bias) of allowing the user to freely alter image processing outcomes needs to be rigorously examined and reported.
- **Blinded image analysis:** Software packages should include built-in support for image filename anonymization to blind the user from an image's study group assignment to minimize bias as images are analyzed.
- **Semi-automated curation:** Image quality and marker expression can change between study groups, which could bias automated segmentation and results. Image analysis programs should, therefore, build on previous efforts[97] to include the option to efficiently curate segmentation within a study group in a blinded fashion in regions where automated analysis fails. While some of the programs allows for a degree of curation with adjusting image processing parameters, there is no examination with how this can bias results if the researcher changes these parameters between study groups or images.
- **Built-in detection of insufficient sampling:** It is important for the image datasets to sample enough of the microvasculature for valid metric quantification. For simple metrics, such as vessel length density or VAF, a simple examination of variance and power analysis can determine whether more images of a biological sample are required. However, for more advanced quantification metrics, such as lacunarity and fractal dimension, or graph theory-based

metrics, the metrics become nonsensical if the field of view is too small and not enough vascular network sampled. These metrics need to be studied and predictive algorithms developed to warn the user if the dataset is at risk for yielding invalid results for advance structural metrics.

- **Source code and dataset availability:** While most published software packages will provide source code and data upon request, we believe that it should be standard to make both freely available for download on long-term hosting platforms such as Github, Bitbucket, or an institutional repository. This removes any barrier to iterate on previous work and facilitates comparison of software packages. Freely available image datasets will also standardize the validation process and enhance progress within the field in the same way standard datasets have with analyzing retina microvessels in fundus imaging.[109,110]

- **Novel metrics:** More metrics need to be developed to describe all observed complexities found in the network structure, with the long-term view that a sufficient number of metrics for characterizing the microvasculature would allow for the successful creation of in silico artificial networks that are indiscernible from experimentally derived microvascular network structures. Any degree short of this reproduction would mean that information is being lost by the current metric set. Techniques for developing new metrics can be guided from the field of feature engineering.[111]

Without tackling these issues, new software programs are merely presented to research scientists "as is" without allowing them to make informed decisions on how to produce high-quality unbiased results. We argue that until these issues are dealt with, the use of these packages has the risk of leading to a significant error rate in microvascular research: where the software reveals a positive error with a quantifiable change between groups where none existed, or even worse, where research is not pursued based on a negative error where no change is observed between study groups where one exists.

4.6 | Applications of machine learning, graph theory, and modeling in quantifying microvascular architecture

Metric effectiveness not only needs to be evaluated on an individual basis, but the effectiveness of a given collection of metrics in combination needs to be evaluated. This can start with examining covariance matrices of metrics from in silico and biological datasets to evaluate how much unique information they bring relative to one another. Effectiveness of metric sets could be evaluated using principal components analysis, partial least squares, or more advanced methods of feature selection techniques from the field of feature engineering,[108] especially when applied to in silico artificial networks where basic parameters (vessel length density, vessel diameter, branchpoints density, tortuosity, connectivity) can be changed in a controlled fashion. Further research must be conducted on what makes an effective metric in an unbiased fashion, and consensus much be reached on normalization of metrics so they can be used in

a standardized way, such as the disagreement on how to normalize branchpoints counts (by image area, vessel length, or binned vessel diameter). This will depend on the development and pairing of fully parametrized in silico models[112] (Table 6), structural models of models of vascular flow,[113,114] and models of predictive tissue oxygenation[115] with biological experiments[116] to fully connect metrics of microvascular structure to biological behaviors.

Blood vessel networks can be abstracted as a series of branchpoints, or nodes, with varying connectivity with each other. Previous work has explored the basic concept of abstracting the microvasculature as a graph,[117] and we believe there are a wealth of relevant metrics that could be applied from quantifying graph networks (Figure 6). Examples include metrics measuring centrality of each node,[118] scoring the relative importance of edges in connecting nodes, connective redundancy,[119] and information diffusion.[120] Machine learning methods such as convolution neural networks and other techniques[121] have also been applied to graph networks.[122] Previous applications of network tomography outside of biomedical research,[123] such as internet tomography,[124] may be a pertinent source of applicable methods for characterizing complex microvascular networks.

4.7 | Relevant techniques from related network architectures

Analysis of full feature microvascular architectures can also benefit from adapting techniques used to analyze similar network structures. A prime example is fundus imaging of human retinal vascular networks: Although such images fail to resolve capillary portions of the microvascular network, this application has been extensively explored due to its established clinical significance in evaluating eye disease and a collection of systemic diseases,[125] with a plethora of methods developed to segment, quantify, and validate vessel architecture.[126] Indeed, a machine learning-based classification pipeline for fundus images has recently been approved by the FDA for diagnosis of diabetic retinopathy.[127] Methods used in the processing and quantification of neuronal network image datasets[128] may yield useful techniques for analyzing microvascular networks.[129] In vivo clinical imaging techniques, such as micro-CT[130] of lung vascular networks, may also yield insight into extending 2D imaging and quantification into the third dimension.[131]

Although this review focuses on 2D image quantification techniques, many of the imaging modalities mentioned acquire data in 3D directly, or through a series of 2D slices. Over the long term, the field would most benefit from acquiring and analyzing 3D datasets to eliminate any confounding phenomena that arises from analyzing a 2D-projected representation of complex 3D structures. Such 2D abstractions can lead to altered metrics, such as false branch points where vessels appear to overlap in 2D but exist at distinct elevations in 3D, introducing error to other metrics such as segment length. Furthermore, the 3D orientation of vessel segments relative to one another is especially important when characterizing local tissue oxygenation.[89] An in-depth examination of how 2D structural metrics can characterize a projected 3D structure like a microvascular

network would also be necessary to understand the trade-offs and reveal what information is missed with this simplification.

4.8 | Statistics to analyze microvascular interactions: beyond generic

The metrics covered in this review require basic 2-sample or multi-sample statistical tests to determine whether there is a difference in structure and morphology of vascular networks between study groups. Yet there are also new statistics being developed based on modeling null distributions (output if the null hypothesis is true and there is no difference between groups) that could be extended to quantifying the microvascular architecture. A prime example of this is a technique to measure cellular recruitment with a given cell type and the vascular network,[132] that maintains validity in conditions where generic statistics fail. While cell recruitment has been analyzed,[97] previous metrics of cell-to-cell colocalization events fails to properly measure changes in cell recruitment if there are changes to vascular density or cell density across study groups. This confounding phenomenon will lead to false positives when testing between study groups[132]: instances where the test indicates there is a significant change in cell recruitment, when in reality there is none. Null modeling of random cell placement is used to avoid the deficiencies of generic statistics, and we believe this modeling approach could be applied to evaluating perivascular cell recruitment to blood vessel architecture using an in silico model and provide researchers with a more robust statistical hypothesis test for analyzing microvessel architecture.

PERSPECTIVES

The microvasculature is implicated in pathogenesis and maintenance of the deadliest maladies of the modern world. Understanding microvasculature's function, adaptation, and contribution to disease is enabled by the application of metrics that quantify changes to microvascular network architecture in in vivo, in vitro, and in silico model systems. We highlight opportunities to further the field by improving scientific rigor and reproducibility through the development and validation of software that reliably, comprehensively, and in an automated manner, characterizes the complexities of microvascular architecture using pre-existing and novel metrics.

ORCID

Bruce A. Corliss (iD) https://orcid.org/0000-0003-2962-7344

REFERENCES

1. Jacob M, Chappell D, Becker BF. Regulation of blood flow and volume exchange across the microcirculation. *Crit Care*. 2016;20:319.
2. Nourshargh S, Alon R. Leukocyte migration into inflamed tissues. *Immunity*. 2014;41(5):694-707.
3. Tonnesen MG, Feng X, Clark RAF. Angiogenesis in wound healing. *J Investig Dermatol Symp Proc*. 2000;5(1):40-46.
4. Chambers R, Zweifach BW. Intercellular cement and capillary permeability. *Physiol Rev*. 1947;27(3):436-463.
5. Pantoni L. Cerebral small vessel disease: from pathogenesis and clinical characteristics to therapeutic challenges. *Lancet Neurol*. 2010;9(7):689-701.
6. Camici PG, Crea F. Coronary microvascular dysfunction. *N Engl J Med*. 2007;356(8):830-840.
7. Tooke JE. Microvascular function in human diabetes. A physiological perspective. *Diabetes*. 1995;44(7):721-726.
8. Centers for Disease Control and Prevention. Deaths: Final Data for 2015. *National Vital Statistics Reports*. 2017; 66(6):75.
9. Zhang H, van Olden C, Sweeney D, Martin-Rendon E. Blood vessel repair and regeneration in the ischaemic heart. *Open Heart*. 2014;1(1):e000016.
10. Ostergaard L, Kristiansen SB, Angleys H, et al. The role of capillary transit time heterogeneity in myocardial oxygenation and ischemic heart disease. *Basic Res Cardiol*. 2014;109(3):409.
11. Rosenkranz S, Gibbs JSR, Wachter R, De Marco T, Vonk-Noordegraaf A, Vachiéry J-L. Left ventricular heart failure and pulmonary hypertension. *Eur Heart J*. 2016;37(12):942-954.
12. Nishida N, Yano H, Nishida T, Kamura T, Kojiro M. Angiogenesis in cancer. *Vasc Health Risk Manag*. 2006;2(3):213-219.
13. García-Román J, Zentella-Dehesa A. Vascular permeability changes involved in tumor metastasis. *Cancer Lett*. 2013;335(2):259-269.
14. Au SH, Storey BD, Moore JC, et al. Clusters of circulating tumor cells traverse capillary-sized vessels. *Proc Natl Acad Sci USA*. 2016;113(18):4947-4952.
15. Voelkel NF, Cool CD. Pulmonary vascular involvement in chronic obstructive pulmonary disease. *Eur Respir J*. 2003;22(46 suppl):28s-32s.
16. Eliason G, Abdel-Halim SM, Piehl-Aulin K, Kadi F. Alterations in the muscle-to-capillary interface in patients with different degrees of chronic obstructive pulmonary disease. *Respir Res*. 2010;11(1):97.
17. Widdicombe JG. Asthma. Tracheobronchial vasculature. *Br Med Bull*. 1992;48(1):108-119.
18. Østergaard L, Jespersen SN, Mouridsen K, et al. The role of the cerebral capillaries in acute ischemic stroke: the extended penumbra model. *J Cereb Blood Flow Metab*. 2013;33(5):635-648.
19. Østergaard L, Jespersen SN, Engedahl T, et al. Capillary dysfunction: its detection and causative role in dementias and stroke. *Curr Neurol Neurosci Rep*. 2015;15(6):37.
20. Yemisci M, Gursoy-Ozdemir Y, Vural A, Can A, Topalkara K, Dalkara T. Pericyte contraction induced by oxidative-nitrative stress impairs capillary reflow despite successful opening of an occluded cerebral artery. *Nat Med*. 2009;15(9):1031-1037.
21. Gjedde A, Kuwabara H, Hakim AM. Reduction of functional capillary density in human brain after stroke. *J Cereb Blood Flow Metab*. 1990;10(3):317-326.
22. Adair TH, Montani J-P. *Overview of Angiogenesis*. Morgan & Claypool Life Sciences; 2010. https://www.ncbi.nlm.nih.gov/books/NBK53238/. Accessed July 30, 2018.
23. Fogelson AL, Neeves KB. Fluid mechanics of blood clot formation. *Annu Rev Fluid Mech*. 2015;47:377-403.
24. Muller WA. Getting leukocytes to the site of inflammation. *Vet Pathol*. 2013;50(1):7-22.
25. Østergaard L, Nagenthiraja K, Gyldensted L, et al. Capillary dysfunction in Alzheimer's disease. *Alzheimers Dement*. 2013;9(4):P269-P270.
26. Hecht M, Krämer LM, von Arnim CAF, Otto M, Thal DR. Capillary cerebral amyloid angiopathy in Alzheimer's disease: association with allocortical/hippocampal microinfarcts and cognitive decline. *Acta Neuropathol*. 2018;135(5):681-694.

27. Beltramo E, Porta M. Pericyte loss in diabetic retinopathy: mechanisms and consequences. *Curr Med Chem*. 2013;20(26):3218-3225.

28. Moldoveanu B, Otmishi P, Jani P, et al. Inflammatory mechanisms in the lung. *J Inflamm Res*. 2008;2:1-11.

29. Gurka DP, Balk RA. Acute respiratory failure. In: Parrillo JE, Dellinger RP, eds. *Critical Care Medicine*, 3rd edn. Philadelphia, PA: Mosby; 2008:773-794. http://www.sciencedirect.com/science/article/pii/B9780323048415500406. Accessed July 30, 2018.

30. Azzi S, Hebda JK, Gavard J. Vascular permeability and drug delivery in cancers. *Front Oncol*. 2013;3:211.

31. Simone E, Ding B-S, Muzykantov V. Targeted delivery of therapeutics to endothelium. *Cell Tissue Res*. 2009;335(1):283-300.

32. Germain RN. Maintaining system homeostasis: the third law of Newtonian immunology. *Nat Immunol*. 2012;13:902-906.

33. Opferman JT, Korsmeyer SJ. Apoptosis in the development and maintenance of the immune system. *Nat Immunol*. 2003;4(5):410-415.

34. Parkin J, Cohen B. An overview of the immune system. *Lancet*. 2001;357(9270):1777-1789.

35. Gramatikov BI. Modern technologies for retinal scanning and imaging: an introduction for the biomedical engineer. *BioMed Eng OnLine*. 2014;13:52.

36. Fabrikant SI, Maggi S, Montello DR. 3D network spatialization: does it add depth to 2D representations of semantic proximity? In: Duckham M, Pebesma E, Stewart K, Frank AU, eds. *Geographic Information Science*. Basel: Springer International Publishing; 2014:34-47. (Lecture Notes in Computer Science).

37. Miolane N, Pennec X. A survey of mathematical structures for extending 2D neurogeometry to 3D image processing; 2015. https://hal.inria.fr/hal-01203518/document. Accessed July 30, 2018.

38. Combs CA. Fluorescence microscopy: a concise guide to current imaging methods. *Curr Protoc Neurosci*. 2010;Chapter 2:Unit2.1.

39. Nuzzo R. Scientific method: statistical errors. *Nature*. 2014;506(7487):150.

40. Bergijk EC, Van Alderwegen IE, Baelde HJ, et al. Differential expression of collagen IV isoforms in experimental glomerulosclerosis. *J Pathol*. 1998;184(3):307-315.

41. Daly SM, Leahy MJ. 'Go with the flow ': a review of methods and advancements in blood flow imaging. *J Biophotonics*. 2013;6(3):217-255.

42. Hoffmann A, Bredno J, Wendland M, Derugin N, Ohara P, Wintermark M. High and low molecular weight fluorescein isothiocyanate (FITC)–dextrans to assess blood-brain barrier disruption: technical considerations. *Transl Stroke Res*. 2011;2(1):106-111.

43. Robertson RT, Levine ST, Haynes SM, et al. Use of labeled tomato lectin for imaging vasculature structures. *Histochem Cell Biol*. 2015;143(2):225-234.

44. Gurevich DB, Severn CE, Twomey C, et al. Live imaging of wound angiogenesis reveals macrophage orchestrated vessel sprouting and regression. *EMBO J*. 2018;4:e97786.

45. Siegenthaler JA, Choe Y, Patterson KP, et al. Foxc1 is required by pericytes during fetal brain angiogenesis. *Biol Open*. 2013;2(7):647-659.

46. Boscia F, Esposito CL, Casamassa A, de Franciscis V, Annunziato L, Cerchia L. The isolectin IB4 binds RET receptor tyrosine kinase in microglia. *J Neurochem*. 2013;126(4):428-436.

47. Allinson KR, Lee HS, Fruttiger M, McCarty J, Arthur HM. Endothelial expression of TGFβ type II receptor is required to maintain vascular integrity during postnatal development of the central nervous system Chen J, editor. *PLoS ONE*. 2012;7(6):e39336.

48. Hu J, Popp R, Frömel T, et al. Müller glia cells regulate Notch signaling and retinal angiogenesis via the generation of 19,20-dihydroxydocosapentaenoic acid. *J Exp Med*. 2014;211(2):281-295.

49. Dominguez E, Raoul W, Calippe B, et al. Experimental branch retinal vein occlusion induces upstream pericyte loss and vascular destabilization. *PLoS ONE*. 2015;10(7):e0132644.

50. Fan J, Ponferrada VG, Sato T, et al. Crim1 maintains retinal vascular stability during development by regulating endothelial cell Vegfa autocrine signaling. *Development (Cambridge, England)*. 2014;141(2):448-459.

51. Lam S, van der Geest RN, Verhagen NAM, Daha MR, van Kooten C. Secretion of collagen type IV by human renal fibroblasts is increased by high glucose via a TGF-beta-independent pathway. *Nephrol Dial Transplant*. 2004;19(7):1694-1701.

52. Baluk P, Morikawa S, Haskell A, Mancuso M, McDonald DM. Abnormalities of basement membrane on blood vessels and endothelial sprouts in tumors. *Am J Pathol*. 2003;163(5):1801-1815.

53. Brown WR. A review of string vessels or collapsed, empty basement membrane tubes. *J Alzheimers Dis*. 2010;21(3):725-739.

54. McVicar CM, Ward M, Colhoun LM, et al. Role of the receptor for advanced glycation endproducts (RAGE) in retinal vasodegenerative pathology during diabetes in mice. *Diabetologia*. 2015;58(5):1129-1137.

55. Yang P, Pavlovic D, Waldvogel H, et al. String vessel formation is increased in the brain of parkinson disease. *J Parkinsons Dis*. 2015;5(4):821-836.

56. Abramsson A, Lindblom P, Betsholtz C. Endothelial and nonendothelial sources of PDGF-B regulate pericyte recruitment and influence vascular pattern formation in tumors. *J Clin Investig*. 2003;112(8):1142-1151.

57. Winkler EA, Sengillo JD, Bell RD, Wang J, Zlokovic BV. Blood–spinal cord barrier pericyte reductions contribute to increased capillary permeability. *J Cereb Blood Flow Metab*. 2012;32(10):1841-1852.

58. Kelly-Goss MR, Sweat RS, Stapor PC, Peirce SM, Murfee WL. Targeting perciytes for angiogenic therapies. *Microcirculation (New York, N.Y. : 1994)*. 2014;21(4):345-357.

59. He L, Vanlandewijck M, Raschperger E, et al. Analysis of the brain mural cell transcriptome. *Sci Rep*. 2016;6:35108.

60. Hughes S, Chan-Ling T. Characterization of smooth muscle cell and pericyte differentiation in the rat retina in vivo. *Invest Ophthalmol Vis Sci*. 2004;45(8):2795-2806.

61. Alarcon-Martinez L, Yilmaz-Ozcan S, Yemisci M, et al. Capillary pericytes express α-smooth muscle actin, which requires prevention of filamentous-actin depolymerization for detection. *eLife*. 2017;7:1-17. https://www.ncbi.nlm.nih.gov/pmc/articles/PMC5862523

62. Cai J, Kehoe O, Smith GM, Hykin P, Boulton ME. The angiopoietin/Tie-2 system regulates pericyte survival and recruitment in diabetic retinopathy. *Invest Opthalmol Vis Sci*. 2008;49(5):2163.

63. Park DY, Lee J, Kim J, et al. Plastic roles of pericytes in the blood–retinal barrier. *Nat Commun*. 2017;8:15296.

64. Teichert M, Milde L, Holm A, et al. Pericyte-expressed Tie2 controls angiogenesis and vessel maturation. *Nat Commun*. 2017;8:16106.

65. Fe Lanfranco M, Loane DJ, Mocchetti I, Burns MP, Villapol S. Combination of fluorescent in situ hybridization (FISH) and immunofluorescence imaging for detection of cytokine expression in microglia/macrophage cells. *Bio Protoc*. 2017;7(22):1-17.

66. Arai F, Hirao A, Ohmura M, et al. Tie2/angiopoietin-1 signaling regulates hematopoietic stem cell quiescence in the bone marrow niche. *Cell*. 2004;118(2):149-161.

67. Patel AS, Smith A, Nucera S, et al. TIE2-expressing monocytes/macrophages regulate revascularization of the ischemic limb. *EMBO Mol Med*. 2013;5(6):858-869.

68. Wolfram JA, Diaconu D, Hatala DA, et al. Keratinocyte but not endothelial cell-specific overexpression of Tie2 leads to the development of psoriasis. *Am J Pathol*. 2009;174(4):1443-1458.

69. Hillen F, Kaijzel EL, Castermans K, oude Egbrink MGA, Löwik CWGM, Griffioen AW. A transgenic Tie2-GFP athymic mouse

model; a tool for vascular biology in xenograft tumors. *Biochem Biophys Res Commun*. 2008;368(2):364-367.

70. Saeidnia S, Manayi A, Abdollahi M. From in vitro experiments to in vivo and clinical studies; pros and cons. *Curr Drug Discov Technol*. 2015;12(4):218-224.

71. Katt ME, Placone AL, Wong AD, Xu ZS, Searson PC. In vitro tumor models: advantages, disadvantages, variables, and selecting the right platform. *Front Bioeng Biotechnol*. 2016;4:12.

72. Holmgaard A, Askou AL, Benckendorff JNE, et al. In vivo knock-out of the vegfa gene by lentiviral delivery of CRISPR/Cas9 in mouse retinal pigment epithelium cells. *Mol Ther Nucleic Acids*. 2017;9:89-99.

73. Crauciuc A, Tripon F, Gheorghiu A, Nemes G, Boglis A, Banescu C. Review. Development, applications, benefits, challenges and limitations of the new genome engineering technique. An update study. *Acta Med Marisiensis*. 2017;63(1):4-9.

74. Wang LV, Gao L. Photoacoustic microscopy and computed tomography: from bench to bedside. *Annu Rev Biomed Eng*. 2014;16(1):155-185.

75. Mahmud MS, Cadotte DW, Vuong B, et al. Review of speckle and phase variance optical coherence tomography to visualize microvascular networks. *J Biomed Optics*. 2013;18(5):050901.

76. Sydor AM, Czymmek KJ, Puchner EM, Mennella V. Super-resolution microscopy: from single molecules to supramolecular assemblies. *Trends Cell Biol*. 2015;25(12):730-748.

77. Dellian M, Witwer BP, Salehi HA, Yuan F, Jain RK. Quantitation and physiological characterization of angiogenic vessels in mice: effect of basic fibroblast growth factor, vascular endothelial growth factor/vascular permeability factor, and host microenvironment. *Am J Pathol*. 1996;149(1):59-71.

78. Zudaire E, Gambardella L, Kurcz C, Vermeren S. A computational tool for quantitative analysis of vascular networks. *PLoS ONE*. 2011;6(11):e27385.

79. Strahler AN. Quantitative analysis of watershed geomorphology. *Trans Am Geophys Union*. 1957;38(6):913.

80. Fenton BM, Zweifach BW. Microcirculatory model relating geometrical variation to changes in pressure and flow rate. *Ann Biomed Eng*. 1981;9(4):303-321.

81. Seaman ME, Peirce SM, Kelly K. Rapid analysis of vessel elements (RAVE): a tool for studying physiologic, pathologic and tumor angiogenesis. *PLoS ONE*. 2011;6(6):e20807.

82. Stamatelos SK, Kim E, Pathak AP, Popel AS. A bioimage informatics based reconstruction of breast tumor microvasculature with computational blood flow predictions. *Microvasc Res*. 2014;91:8-21.

83. Niemisto A, Dunmire V, Yli-Harja O, Zhang W, Shmulevich I. Robust quantification of in vitro angiogenesis through image analysis. *IEEE Trans Med Imaging*. 2005;24(4):549-553.

84. Sové RJ, Goldman D, Fraser GM. A computational model of the effect of capillary density variability on oxygen transport, glucose uptake, and insulin sensitivity in prediabetes. *Microcirculation*. 2017;24(2):e12342.

85. Nolan DJ, Ginsberg M, Israely E, et al. Molecular signatures of tissue-specific microvascular endothelial cell heterogeneity in organ maintenance and regeneration. *Dev Cell*. 2013;26(2):204-219.

86. Chi J-T, Chang HY, Haraldsen G, et al. Endothelial cell diversity revealed by global expression profiling. *Proc Natl Acad Sci USA*. 2003;100(19):10623-10628.

87. Banavar JR, Cooke TJ, Rinaldo A, Maritan A. Form, function, and evolution of living organisms. *Proc Natl Acad Sci*. 2014;111(9):3332-3337.

88. Fraser GM, Goldman D, Ellis CG. Comparison of generated parallel capillary arrays to three-dimensional reconstructed capillary networks in modeling oxygen transport in discrete microvascular volumes. *Microcirculation (New York, N.Y.: 1994)*. 2013;20(8):748-763.

89. Fraser GM, Goldman D, Ellis CG. Microvascular flow modeling using in vivo hemodynamic measurements in reconstructed 3D capillary networks. *Microcirculation (New York, N.Y.: 1994)*. 2012;19(6):510-520.

90. Davis GE, Norden PR, Bowers SLK. Molecular control of capillary morphogenesis and maturation by recognition and remodeling of the extracellular matrix: functional roles of endothelial cells and pericytes in health and disease. *Connect Tissue Res*. 2015;56(5):392-402.

91. Han H-C. Twisted blood vessels: symptoms, etiology and biomechanical mechanisms. *J Vasc Res*. 2012;49(3):185-197.

92. Tykocki NR, Boerman EM, Jackson WF. Smooth muscle ion channels and regulation of vascular tone in resistance arteries and arterioles. *Compr Physiol*. 2017;7(2):485-581.

93. Hamilton NB, Attwell D, Hall CN. Pericyte-mediated regulation of capillary diameter: a component of neurovascular coupling in health and disease. *Front Neuroenergetics*. 2010;2:1-15. https://www.frontiersin.org/articles/10.3389/fnene.2010.00005/full

94. Carroll RG. *Elsevier's Integrated Physiology*. Philadelphia, PA: Mosby Elsevier; 2007.

95. Granger DN, Senchenkova E. *Inflammation and the Microcirculation*. San Rafael, CA: Morgan & Claypool Life Sciences; 2010. (Integrated Systems Physiology—From Cell to Function).

96. Pfister F, Feng Y, vom Hagen F, et al. Pericyte migration: a novel mechanism of pericyte loss in experimental diabetic retinopathy. *Diabetes*. 2008;57(9):2495-2502.

97. Morin KT, Carlson PD, Tranquillo RT. Automated image analysis programs for the quantification of microvascular network characteristics. *Methods (San Diego, Calif.)*. 2015;84:76-83.

98. Ding L, Cheng R, Hu Y, et al. Peroxisome proliferator–activated receptor α protects capillary pericytes in the retina. *Am J Pathol*. 2014;184(10):2709-2720.

99. Shami A, Knutsson A, Dunér P, et al. Dystrophin deficiency reduces atherosclerotic plaque development in ApoE-null mice. *Sci Rep*. 2015;5(1):13904.

100. Seaman SA, Cao Y, Campbell CA, Peirce SM. Macrophage recruitment and polarization during collateral vessel remodeling in murine adipose tissue. *Microcirculation (New York, N.Y.: 1994)*. 2016;23(1):75-87.

101. Corliss BA, Azimi MS, Munson JM, Peirce SM, Murfee WL. Macrophages: an inflammatory link between angiogenesis and lymphangiogenesis. *Microcirculation (New York, N.Y.: 1994)*. 2016;23(2):95-121.

102. Wu J, Hadoke PW, Takov K, Korczak A, Denvir M, Smith L. Influence of androgen receptor in vascular cells on reperfusion following hindlimb ischaemia. *PLoS ONE*. 2016;11:e0154987.

103. Rueden CT, Schindelin J, Hiner MC, et al. Image J2: ImageJ for the next generation of scientific image data. *BMC Bioinformatics*. 2017;18:529.

104. Schindelin J, Arganda-Carreras I, Frise E, et al. Fiji: an open-source platform for biological-image analysis. *Nat Methods*. 2012;9(7):676-682.

105. Manjunathan R, Ragunathan M. Chicken chorioallantoic membrane as a reliable model to evaluate osteosarcoma—an experimental approach using SaOS2 cell line. *Biol Proced Online*. 2015;17:10.

106. Sprindzuk M, Dmitruk A, Kovalev V, et al. Computer-aided image processing of angiogenic histological. *J Clin Med Res*. 2009;1(5):249-261.

107. Peirce SM. Computational and mathematical modeling of angiogenesis. *Microcirculation (New York, N.Y.: 1994)*. 2008;15(8):739-751.

108. Hira ZM, Gillies DF. A review of feature selection and feature extraction methods applied on microarray data. *Adv Bioinformatics*. 2015;2015:1-13.

109. Hoover AD, Kouznetsova V, Goldbaum M. Locating blood vessels in retinal images by piecewise threshold probing of a matched filter response. *IEEE Trans Med Imaging*. 2000;19(3):203-210.

110. Staal J, Abramoff MD, Niemeijer M, Viergever MA, van Ginneken B. Ridge-based vessel segmentation in color images of the retina. *IEEE Trans Med Imaging*. 2004;23(4):501-509.

111. Goel R, Kumar V, Srivastava S, Sinha AK. A review of feature extraction techniques for image analysis. *IJARCET*. 2017;6(2):3.

112. Pries AR, Secomb TW. Making microvascular networks work: angiogenesis, remodeling, and pruning. *Physiology*. 2014;29(6):446-455.

113. Fry BC, Lee J, Smith NP, Secomb TW. Estimation of blood flow rates in large microvascular networks. *Microcirculation*. 2012;19(6):530-538.

114. Secomb TW. Theoretical models for regulation of blood flow. *Microcirculation*. 2015;15(8):765-775.

115. Gould IG, Linninger AA. Hematocrit distribution and tissue oxygenation in large microcirculatory networks. *Microcirculation*. 2015;22(1):1-18.

116. Kuliga KZ, McDonald EF, Gush R, Michel C, Chipperfield AJ, Clough GF. Dynamics of microvascular blood flow and oxygenation measured simultaneously in human skin. *Microcirculation*. 2014;21(6):562-573.

117. Paradowski M, Kwasnicka H, Borysewicz K. Capillary blood vessel tortuosity measurement using graph analysis. In: Setchi R, Jordanov I, eds.*Knowledge-Based and Intelligent Information and Engineering Systems*. Berlin, Heidelberg: Springer; 2009:135-142. (Lecture Notes in Computer Science).

118. Vargas R, Waldron A, Sharma A, Flórez R, Narayan DA. A graph theoretic analysis of leverage centrality. *AKCE Int J Graphs Comb*. 2017;14(3):295-306.

119. Di Lanzo C, Marzetti L, Zappasodi F, De Vico Fallani F, Pizzella V. Redundancy as a graph-based index of frequency specific MEG functional connectivity. *Comput Math Methods Med*. 2012;2012:207305.

120. Malliaros FD, Rossi M-EG, Vazirgiannis M. Locating influential nodes in complex networks. *Sci Rep*. 2016;6:19307.

121. Zhang W, Chien J, Yong J, Kuang R. Network-based machine learning and graph theory algorithms for precision oncology. *NPJ Precis Oncol*. 2017;1(1):25.

122. Niepert M, Ahmed M, Kutzkov K. Learning Convolutional Neural Networks for Graphs. Proceedings of The 33rd International Conference on Machine Learning, in PMLR 48 2016:2014-2023.

123. Lawrence E, Michailidis G, Nair VN, Xi B. Network tomography: a review and recent developments. In: Fan J, Koul H, eds. *Frontiers in Statistics*. London: Imperial College Press; 2006:345-366.

124. Coates A, Hero AO III, Nowak R, Yu B. Internet tomography. *IEEE Signal Process Mag*. 2002;19(3):47-65.

125. Abramoff MD, Garvin MK, Sonka M. Retinal imaging and image analysis. *IEEE Rev Biomed Eng*. 2010;3:169-208.

126. Trucco E, Ruggeri A, Karnowski T, et al. Validating retinal fundus image analysis algorithms: issues and a proposal. *Invest Ophthalmol Vis Sci*. 2013;54(5):3546-3559.

127. van der Heijden AA, Abramoff MD, Verbraak F, van Hecke MV, Liem A, Nijpels G. Validation of automated screening for referable diabetic retinopathy with the IDx-DR device in the Hoorn Diabetes Care System. *Acta Ophthalmol*. 2018;96(1):63-68.

128. Batabyal T, Vaccari A, Acton ST. NeuroBFD: Size-independent automated classification of neurons using conditional distributions of morphological features. In: 2018 IEEE 15th International Symposium on Biomedical Imaging (ISBI 2018); 2018:912-915.

129. Batabyal T, Acton ST. ElasticPath2Path: Automated morphological classification of neurons by elastic path matching. arXiv:1802.06913 [eess, q-bio]; 2018. http://arxiv.org/abs/1802.06913. Accessed August 22. 2018

130. Vasquez SX, Gao F, Su F, et al. Optimization of MicroCT imaging and blood vessel diameter quantitation of preclinical specimen vasculature with radiopaque polymer injection medium. *PLoS ONE*. 2011;6(4):e19099.

131. Bruyninckx P, Loeckx D, Vandermeulen D, Suetens P. Segmentation of lung vessel trees by global optimization. In: Pluim JPW, Dawant BM, eds. . Proceedings of SPIE 7259, Medical ImagingLake Buena Vista, FL; 2009.

132. Corliss BA, Ray HC, Patrie J, et al. CIRCOAST: a statistical hypothesis test for cellular colocalization with network structures. *Bioinformatics*. 2018;1-9.

133. Stintzing S, Ocker M, Hartner A, Amann K, Barbera L, Neureiter D. Differentiation patterning of vascular smooth muscle cells (VSMC) in atherosclerosis. *Virchows Arch*. 2009;455(2):171-185.

134. Liu L, Shi G-P. CD31: beyond a marker for endothelial cells. *Cardiovasc Res*. 2012;94(1):3-5.

135. Yu QC, Song W, Wang D, Zeng YA. Identification of blood vascular endothelial stem cells by the expression of protein C receptor. *Cell Res*. 2016;26(10):1079-1098.

136. Kumar A, D'Souza SS, Moskvin OV, et al. Specification and diversification of pericytes and smooth muscle cells from mesenchymoangioblasts. *Cell Rep*. 2017;19(9):1902-1916.

137. Fang X, Djouhri L, McMullan S, et al. Intense isolectin-B4 binding in rat dorsal root ganglion neurons distinguishes C-fiber nociceptors with broad action potentials and high Nav1.9 expression. *J Neurosci*. 2006;26(27):7281-7292.

138. Kubo A, Katanosaka K, Mizumura K. Extracellular matrix proteoglycan plays a pivotal role in sensitization by low pH of mechanosensitive currents in nociceptive sensory neurones. *J Physiol*. 2012;590(13):2995-3007.

139. Ismail JA, Poppa V, Kemper LE, et al. Immunohistologic labeling of murine endothelium. *Cardiovasc Pathol*. 2003;12(2):82-90.

140. Zakharova IS, Zhiven' MK, Saaya SB, et al. Endothelial and smooth muscle cells derived from human cardiac explants demonstrate angiogenic potential and suitable for design of cell-containing vascular grafts. *J Transl Med*. 2017;15:54.

141. Lünemann A, Ullrich O, Diestel A, et al. Macrophage/microglia activation factor expression is restricted to lesion-associated microglial cells after brain trauma. *Glia*. 2006;53(4):412-419.

142. Wattananit S, Tornero D, Graubardt N, et al. Monocyte-derived macrophages contribute to spontaneous long-term functional recovery after stroke in mice. *J Neurosci*. 2016;36(15):4182-4195.

143. Bahramsoltani M, Slosarek I, De Spiegelaere W, Plendl J. Angiogenesis and collagen type IV expression in different endothelial cell culture systems. *Anat Histol Embryol*. 2014;43(2):103-115.

144. Sava P, Cook IO, Mahal RS, Gonzalez AL. Human microvascular pericyte basement membrane remodeling regulates neutrophil recruitment. *Microcirculation*. 2015;22(1):54-67.

145. Katsuda S, Okada Y, Minamoto T, Nakanishi I. Enhanced synthesis of type IV collagen in cultured arterial smooth muscle cells associated with phenotypic modulation by dimethyl sulfoxide. *Cell Biol Int Rep*. 1987;11(12):861-870.

146. Feru J, Delobbe E, Ramont L, et al. Aging decreases collagen IV expression in vivo in the dermo-epidermal junction and in vitro in dermal fibroblasts: possible involvement of TGF-β1. *Eur J Dermatol*. 2016;26(4):350-360.

147. Sillat T, Saat R, Pöllänen R, Hukkanen M, Takagi M, Konttinen YT. Basement membrane collagen type IV expression by human mesenchymal stem cells during adipogenic differentiation. *J Cell Mol Med*. 2012;16(7):1485-1495.

148. Kim H, Yoon CS, Kim H, Rah B. Expression of extracellular matrix components fibronectin and laminin in the human fetal heart. *Cell Struct Funct*. 1999;24(1):19-26.

149. Yousif LF, Di Russo J, Sorokin L. Laminin isoforms in endothelial and perivascular basement membranes. *Cell Adh Migr*. 2013;7(1):101-110.

150. Godin LM, Sandri BJ, Wagner DE, et al. Decreased laminin expression by human lung epithelial cells and fibroblasts cultured in acellular lung scaffolds from aged mice. *PLoS ONE*. 2016;11(3):e0150966.

151. Ekblom M, Falk M, Salmivirta K, Durbeej M, Ekblom P. Laminin isoforms and epithelial development. *Ann N Y Acad Sci*. 1998;857:194-211.

152. Fina L, Molgaard HV, Robertson D, et al. Expression of the CD34 gene in vascular endothelial cells. *Blood*. 1990;75(12):2417-2426.

153. Armulik A, Genové G, Betsholtz C. Pericytes: developmental, physiological, and pathological perspectives, problems, and promises. *Dev Cell*. 2011;21(2):193-215.

154. Hindle P, Khan N, Biant L, Péault B. The infrapatellar fat pad as a source of perivascular stem cells with increased chondrogenic potential for regenerative medicine. *Stem Cells Transl Med*. 2017;6(1):77-87.

155. Sidney LE, Branch MJ, Dunphy SE, Dua HS, Hopkinson A. Concise review: evidence for CD34 as a common marker for diverse progenitors. *Stem Cells (Dayton, Ohio)*. 2014;32(6):1380-1389.

156. Giampietro C, Taddei A, Corada M, et al. Overlapping and divergent signaling pathways of N-cadherin and VE-cadherin in endothelial cells. *Blood*. 2012;119(9):2159-2170.

157. Chang L, Noseda M, Higginson M, et al. Differentiation of vascular smooth muscle cells from local precursors during embryonic and adult arteriogenesis requires Notch signaling. *Proc Natl Acad Sci*. 2012;109(18):6993-6998.

158. Gavard J. Endothelial permeability and VE-cadherin. *Cell Adh Migr*. 2014;8(2):158-164.

159. Zahr A, Alcaide P, Yang J, et al. Endomucin prevents leukocyte–endothelial cell adhesion and has a critical role under resting and inflammatory conditions. *Nat Commun*. 2016;7:10363.

160. Liu C, Shao ZM, Zhang L, et al. Human endomucin is an endothelial marker. *Biochem Biophys Res Commun*. 2001;288(1):129-136.

161. Samulowitz U, Kuhn A, Brachtendorf G, et al. Human endomucin. *Am J Pathol*. 2002;160(5):1669-1681.

162. Brachtendorf G, Kuhn A, Samulowitz U, et al. Early expression of endomucin on endothelium of the mouse embryo and on putative hematopoietic clusters in the dorsal aorta. *Dev Dyn*. 2001;222(3):410-419.

163. Zanetta L, Marcus SG, Vasile J, et al. Expression of Von Willebrand factor, an endothelial cell marker, is up-regulated by angiogenesis factors: a potential method for objective assessment of tumor angiogenesis. *Int J Cancer*. 2000;85(2):281-288.

164. Trost A, Lange S, Schroedl F, et al. Brain and retinal pericytes: origin, function and role. *Front Cell Neurosci*. 2016;10:20.

165. Balabanov R, Dore-Duffy P. Role of the CNS microvascular pericyte in the blood-brain barrier. *J Neurosci Res*. 1998;53(6):637-644.

166. Strauss O, Phillips A, Ruggiero K, Bartlett A, Dunbar PR. Immunofluorescence identifies distinct subsets of endothelial cells in the human liver. *Sci Rep*. 2017;7:44356.

167. Bergers G, Song S. The role of pericytes in blood-vessel formation and maintenance. *Neuro Oncol*. 2005;7(4):452-464.

168. Merkulova-Rainon T, Broqueres-You D, Kubis N, Silvestre J-S, Levy BI. Towards the therapeutic use of vascular smooth muscle progenitor cells. *Cardiovasc Res*. 2012;95(2):205-214.

169. Hinz B, Celetta G, Tomasek JJ, Gabbiani G, Chaponnier C. Alpha-smooth muscle actin expression upregulates fibroblast contractile activity. *Mol Biol Cell*. 2001;12(9):2730-2741.

170. Lindskog H, Athley E, Larsson E, Lundin S, Hellström M, Lindahl P. New insights to vascular smooth muscle cell and pericyte differentiation of mouse embryonic stem cells in vitro. *Arterioscler Thromb Vasc Biol*. 2006;26(7):1457-1464.

171. Haskins RM, Nguyen AT, Alencar GF, et al. Klf4 has an unexpected protective role in perivascular cells within the microvasculature. *Am J Physiol Heart Circ Physiol*. 2018;315:H402-H414.

172. Shankman LS, Gomez D, Cherepanova OA, et al. KLF4 dependent phenotypic modulation of SMCs plays a key role in atherosclerotic plaque pathogenesis. *Nat Med*. 2015;21(6):628-637.

173. Fukushi J, Makagiansar IT, Stallcup WB. NG2 proteoglycan promotes endothelial cell motility and angiogenesis via engagement of galectin-3 and α3β1 integrin. *Mol Biol Cell*. 2004;15(8):3580-3590.

174. Zhu L, Xiang P, Guo K, et al. Microglia/monocytes with NG2 expression have no phagocytic function in the cortex after LPS focal injection into the rat brain. *Glia*. 2012;60(9):1417-1426.

175. Yan X, Yan L, Liu S, Shan Z, Tian Y, Jin Z. N-cadherin, a novel prognostic biomarker, drives malignant progression of colorectal cancer. *Mol Med Rep*. 2015;12(2):2999-3006.

176. Tsuchiya B, Sato Y, Kameya T, Okayasu I, Mukai K. Differential expression of N-cadherin and E-cadherin in normal human tissues. *Arch Histol Cytol*. 2006;69(2):135-145.

177. Sun Z, Parrish AR, Hill MA, Meininger GA. N-cadherin, a vascular smooth muscle cell-cell adhesion molecule: function and signaling for vasomotor control. *Microcirculation*. 2014;21(3):208-218.

178. Ishimine H, Yamakawa N, Sasao M, et al. N-Cadherin is a prospective cell surface marker of human mesenchymal stem cells that have high ability for cardiomyocyte differentiation. *Biochem Biophys Res Commun*. 2013;438(4):753-759.

179. Council L, Hameed O. Differential expression of immuno-histochemical markers in bladder smooth muscle and myofibroblasts, and the potential utility of desmin, smoothelin, and vimentin in staging of bladder carcinoma. *Mod Pathol*. 2009;22(5):639-650.

180. Gerhardt H, Betsholtz C. Endothelial-pericyte interactions in angiogenesis. *Cell Tissue Res*. 2003;314(1):15-23.

181. Hewitt KJ, Shamis Y, Knight E, et al. PDGFRβ expression and function in fibroblasts derived from pluripotent cells is linked to DNA demethylation. *J Cell Sci*. 2012;125(9):2276-2287.

182. Lindblom P, Gerhardt H, Liebner S, et al. Endothelial PDGF-B retention is required for proper investment of pericytes in the microvessel wall. *Genes Dev*. 2003;17(15):1835-1840.

183. Damisah EC, Hill RA, Tong L, Murray KN, Grutzendler J. A fluoro-Nissl dye identifies pericytes as distinct vascular mural cells during in vivo brain imaging. *Nat Neurosci*. 2017;20(7):1023-1032.

184. Hill M, Davis M. *Local Control of Microvascular Perfusion*. San Rafael, CA: Morgan & Claypool Publishers; 2012.

185. Clemetson KJ, Clemetson JM. Platelet receptors A2. In: Michelson AD, ed. *Platelets*, 3rd edn. San Diego, CA: Academic Press; 2013:169-194.

186. Fukuhara S, Sako K, Noda K, Nagao K, Miura K, Mochizuki N. Tie2 is tied at the cell-cell contacts and to extracellular matrix by Angiopoietin-1. *Exp Mol Med*. 2009;41(3):133-139.

187. Ito K, Turcotte R, Cui J, et al. Self-renewal of a purified Tie2+ hematopoietic stem cell population relies on mitochondrial clearance. *Science (New York, N.Y.)*. 2016;354(6316):1156-1160.

188. Li S, Li T, Luo Y, et al. Retro-orbital injection of FITC-dextran is an effective and economical method for observing mouse retinal vessels. *Mol Vis*. 2011;17:3566-3573.

189. Roberts JJ, Martens PJ. Engineering biosynthetic cell encapsulation systems. In: Poole-Warren L, Martens P, Green R, eds. *Biosynthetic Polymers for Medical Applications*. London: Woodhead Publishing; 2016:205-239. (Woodhead Publishing Series in Biomaterials).

190. Kappel A, Rönicke V, Damert A, Flamme I, Risau W, Breier G. Identification of vascular endothelial growth factor (VEGF) receptor-2 (Flk-1) promoter/enhancer sequences sufficient for angioblast and endothelial cell-specific transcription in transgenic mice. *Blood*. 1999;93(12):4284-4292.

191. Haruta H, Nagata Y, Todokoro K. Role of Flk-1 in mouse hematopoietic stem cells. *FEBS Lett*. 2001;507(1):45-48.

192. Choi J-S, Kim H-Y, Cha J-H, et al. Upregulation of vascular endothelial growth factor receptors Flt-1 and Flk-1 following acute spinal cord contusion in rats. *J Histochem Cytochem*. 2007;55(8):821-830.

193. Yang S-Z, Zhang L-M, Huang Y-L, Sun F-Y. Distribution of Flk-1 and Flt-1 receptors in neonatal and adult rat brains. *Anat Rec A Discov Mol Cell Evol Biol*. 2003;274(1):851-856.

194. Miettinen M, Rikala M-S, Rysz J, Lasota J, Wang Z-F. Vascular endothelial growth factor receptor 2 (VEGFR2) as a marker for malignant vascular tumors and mesothelioma – immunohistochemical study of 262 vascular endothelial and 1640 nonvascular tumors. *Am J Surg Pathol*. 2012;36(4):629-639.

195. Eilken HM, Diéguez-Hurtado R, Schmidt I, et al. Pericytes regulate VEGF-induced endothelial sprouting through VEGFR1. *Nat Commun*. 2017;8(1):1574.

196. Motoike T, Loughna S, Perens E, et al. Universal GFP reporter for the study of vascular development. *Genesis (New York, N.Y.: 2000)*. 2000;28(2):75-81.

197. Cha YR, Weinstein BM. Visualization and experimental analysis of blood vessel formation using transgenic zebrafish. *Birth Defects Res C Embryo Today*. 2007;81(4):286-296.

198. Kisanuki YY, Hammer RE, Miyazaki J, Williams SC, Richardson JA, Yanagisawa M. Tie2-Cre transgenic mice: a new model for endothelial cell-lineage analysis in vivo. *Dev Biol*. 2001;230(2):230-242.

199. Constien R, Forde A, Liliensiek B, et al. Characterization of a novel EGFP reporter mouse to monitor Cre recombination as demonstrated by a Tie2 Cre mouse line. *Genesis (New York, N.Y.: 2000)*. 2001;30(1):36-44.

200. Forde A, Constien R, Gröne H-J, Hämmerling G, Arnold B. Temporal Cre-mediated recombination exclusively in endothelial cells using Tie2 regulatory elements. *Genesis*. 2002;33(4):191-197.

201. Hartmann DA, Underly RG, Watson AN, Shih AY. A murine toolbox for imaging the neurovascular unit. *Microcirculation (New York, N.Y. : 1994)*. 2015;22(3):168-182.

202. Alva JA, Zovein AC, Monvoisin A, et al. VE-Cadherin-Cre-recombinase transgenic mouse: a tool for lineage analysis and gene deletion in endothelial cells. *Dev Dyn*. 2006;235(3):759-767.

203. Chen Q, Zhang H, Liu Y, et al. Endothelial cells are progenitors of cardiac pericytes and vascular smooth muscle cells. *Nat Commun*. 2016;7:12422.

204. Zhong W, Gao X, Wang S, et al. Prox1-GFP/Flt1-DsRed transgenic mice: an animal model for simultaneous live imaging of angiogenesis and lymphangiogenesis. *Angiogenesis*. 2017;20(4):581-598.

205. Lawson ND, Weinstein BM. In vivo imaging of embryonic vascular development using transgenic zebrafish. *Dev Biol*. 2002;248(2):307-318.

206. Poché RA, Larina IV, Scott ML, Saik JE, West JL, Dickinson ME. The Flk1-myr:mCherry mouse as a useful reporter to characterize multiple aspects of ocular blood vessel development and disease. *Dev Dyn*. 2009;238(9):2318-2326.

207. Jin S-W, Herzog W, Santoro MM, et al. A transgene-assisted genetic screen identifies essential regulators of vascular development in vertebrate embryos. *Dev Biol*. 2007;307(1):29-42.

208. Larina IV, Shen W, Kelly OG, Hadjantonakis A-K, Baron MH, Dickinson ME. A membrane associated mCherry fluorescent reporter line for studying vascular remodeling and cardiac function during murine embryonic development. *Anat Rec (Hoboken, N.J.: 2007)*. 2009;292(3):333-341.

209. Cuervo H, Pereira B, Nadeem T, et al. PDGFRβ-P2A-CreERT2 mice: a genetic tool to target pericytes in angiogenesis. *Angiogenesis*. 2017;20(4):655-662.

210. Zhu X, Bergles DE, Nishiyama A. NG2 cells generate both oligodendrocytes and gray matter astrocytes. *Development*. 2008;135(1):145-157.

211. Volz KS, Jacobs AH, Chen HI, et al. Pericytes are progenitors for coronary artery smooth muscle. *eLife*. 2015;4:1-22.

212. Iljin K, Petrova TV, Veikkola T, Kumar V, Poutanen M, Alitalo K. A fluorescent Tie1 reporter allows monitoring of vascular development and endothelial cell isolation from transgenic mouse embryos. *FASEB J*. 2002;16(13):1764-1774.

213. Claxton S, Kostourou V, Jadeja S, Chambon P, Hodivala-Dilke K, Fruttiger M. Efficient, inducible Cre-recombinase activation in vascular endothelium. *Genesis (New York, N.Y.: 2000)*. 2008;46(2):74-80.

214. Fernández-Klett F, Offenhauser N, Dirnagl U, Priller J, Lindauer U. Pericytes in capillaries are contractile in vivo, but arterioles mediate functional hyperemia in the mouse brain. *Proc Natl Acad Sci USA*. 2010;107(51):22290-22295.

215. Proebstl D, Voisin M-B, Woodfin A, et al. Pericytes support neutrophil subendothelial cell crawling and breaching of venular walls in vivo. *J Exp Med*. 2012;209(6):1219-1234.

216. Yokota T, Kawakami Y, Nagai Y, et al. Bone marrow lacks a transplantable progenitor for smooth muscle type alpha-actin-expressing cells. *Stem Cells (Dayton, Ohio)*. 2006;24(1):13-22.

217. Wendling O, Bornert J-M, Chambon P, Metzger D. Efficient temporally-controlled targeted mutagenesis in smooth muscle cells of the adult mouse. *Genesis (New York, N.Y.: 2000)*. 2009;47(1):14-18.

218. Nguyen M, Shing Y, Folkman J. Quantitation of angiogenesis and antiangiogenesis in the chick embryo chorioallantoic membrane. *Microvasc Res*. 1994;47(1):31-40.

219. Gavins FNE, Chatterjee BE. Intravital microscopy for the study of mouse microcirculation in anti-inflammatory drug research: focus on the mesentery and cremaster preparations. *J Pharmacol Toxicol Methods*. 2004;49(1):1-14.

220. Boerman EM, Segal SS. Depressed perivascular sensory innervation of mouse mesenteric arteries with advanced age. *J Physiol*. 2016;594(8):2323-2338.

221. Lipowsky HH, Zweifach BW. Network analysis of microcirculation of cat mesentery. *Microvasc Res*. 1974;7(1):73-83.

222. Sinkler SY, Segal SS. Aging alters reactivity of microvascular resistance networks in mouse gluteus maximus muscle. *Am J Physiol Heart Circ Physiol*. 2014;307(6):H830-H839.

223. Socha MJ, Segal SS. Isolation of microvascular endothelial tubes from mouse resistance arteries. *J Vis Exp*. 2013;81:e50759.

224. Jackson WF, Huebner JM, Rusch NJ. Enzymatic isolation and characterization of single vascular smooth muscle cells from cremasteric arterioles. *Microcirculation (New York, N.Y.: 1994)*. 1997;4(1):35-50.

225. Asai A, Sahani N, Ouchi Y, Martyn J, Yasuhara S. In vivo microcirculation measurement in skeletal muscle by intra-vital microscopy. *J Vis Exp*. 2007;4:210.

226. Menth-Chiari WA, Curl WW, Rosencrance E, Smith TL. Contusion of skeletal muscle increases leukocyte-endothelial cell interactions: an intravital-microscopy study in rats. *J Trauma*. 1998;45(4):709-714.

227. Bagher P, Segal SS. The mouse cremaster muscle preparation for intravital imaging of the microcirculation. *J Vis Exp*. 2011;(52):https://doi.org/10.3791/2874.

228. Gaber MW, Yuan H, Killmar JT, Naimark MD, Kiani MF, Merchant TE. An intravital microscopy study of radiation-induced changes in permeability and leukocyte–endothelial cell interactions in the microvessels of the rat pia mater and cremaster muscle. *Brain Res Protoc*. 2004;13(1):1-10.

229. Eisen JS, Smith JC. Controlling morpholino experiments: don't stop making antisense. *Development*. 2008;135(10):1735-1743.

230. Coonrod SA, Bolling LC, Wright PW, Visconti PE, Herr JC. A morpholino phenocopy of the mouse MOS mutation. *Genesis*. 2001;30(3):198-200.

231. Clark ER. Studies on the growth of blood-vessels in the tail of the frog larva—by observation and experiment on the living animal. *Am J Anat*. 1918;23(1):37-88.

232. Kelly-Goss MR, Ning B, Bruce AC, et al. Dynamic, heterogeneous endothelial Tie2 expression and capillary blood flow during microvascular remodeling. *Sci Rep*. 2017;7(1):9049.

233. van Duinen V, Trietsch SJ, Joore J, Vulto P, Hankemeier T. Microfluidic 3D cell culture: from tools to tissue models. *Curr Opin Biotechnol*. 2015;35:118-126.

234. Sánchez-Palencia DM, Bigger-Allen A, Saint-Geniez M, Arboleda-Velásquez JF, D'Amore PA. Coculture assays for endothelial cells-mural cells interactions. *Methods Mol Biol (Clifton, N.J.)*. 2016;1464:35-47.

235. Waters J, Kluger M, Graham M, Chang W, Bradley J, Pober J. In vitro self-assembly of human pericyte-supported endothelial microvessels in three-dimensional co-culture: a simple model for interrogating endothelial:pericyte interactions. *J Vascular Res*. 2013;50(4):324-331.

236. Stahl A, Connor KM, Sapieha P, et al. The mouse retina as an angiogenesis model. *Invest Ophthalmol Vis Sci*. 2010;51(6):2813-2826.

237. Jackson M, Taylor AH, Jones EA, Forrester LM. The culture of mouse embryonic stem cells and formation of embryoid bodies. *Methods Mol Biol (Clifton, N.J.)*. 2010;633:1-18.

238. Humpel C. Organotypic brain slice cultures: a review. *Neuroscience*. 2015;305:86-98.

239. Johnson TV, Martin KR. Development and characterization of an adult retinal explant organotypic tissue culture system as an in vitro intraocular stem cell transplantation model. *Invest Ophthalmol Vis Sci*. 2008;49(8):3503-3512.

240. Sawamiphak S, Ritter M, Acker-Palmer A. Preparation of retinal explant cultures to study ex vivo tip endothelial cell responses. *Nat Protoc*. 2010;5(10):1659-1665.

241. Bull N, Johnson T, Martin K. Organotypic explant culture of adult rat retina for in vitro investigations of neurodegeneration, neuroprotection and cell transplantation; 2011. https://www.nature.com/protocolexchange/protocols/2042. Accessed July 20, 2018.

242. Downs KM, Temkin R, Gifford S, McHugh J. Study of the murine allantois by allantoic explants. *Dev Biol*. 2001;233(2):347-364.

243. Nakatsu MN, Hughes CCW. An optimized three-dimensional in vitro model for the analysis of angiogenesis. *Methods Enzymol*. 2008;443:65-82.

244. Huang B, Babcock H, Zhuang X. Breaking the diffraction barrier: super-resolution imaging of cells. *Cell*. 2010;143(7):1047-1058.

245. Thorn K. A quick guide to light microscopy in cell biology. *Mol Biol Cell*. 2016;27(2):219-222.

246. Heintzmann R, Ficz G. Breaking the resolution limit in light microscopy. *Brief Funct Genomics*. 2006;5(4):289-301.

247. Fernández-Suárez M, Ting AY. Fluorescent probes for super-resolution imaging in living cells. *Nat Rev Mol Cell Biol*. 2008;9(12):929-943.

248. Graf BW, Boppart SA. Imaging and analysis of three-dimensional cell culture models. *Methods Mol Biol (Clifton, N.J.)*. 2010;591:211-227.

249. Jonkman J, Brown CM. Any way you slice it—a comparison of confocal microscopy techniques. *J Biomol Tech*. 2015;26(2):54-65.

250. Carter M, Shieh J. Microscopy. In: Carter M, Shieh J, eds. *Guide to Research Techniques in Neuroscience*, 2nd edn. San Diego, CA: Academic Press; 2015:117-144.

251. Helmchen F, Denk W. Deep tissue two-photon microscopy. *Nat Methods*. 2005;2(12):932-940.

252. Patterson GH, Piston DW. Photobleaching in two-photon excitation microscopy. *Biophys J* . 2000;78(4):2159-2162.

253. Xia J, Yao J, Wang LV. Photoacoustic tomography: principles and advances. *Electromagn Waves (Cambridge, Mass.)*. 2014;147:1-22.

254. Wang L, Maslov K, Xing W, Garcia-Uribe A, Wang LV. Video-rate functional photoacoustic microscopy at depths. *J Biomed Optics*. 2012;17(10):106007.

255. Xu M, Wang LV. Photoacoustic imaging in biomedicine. *Rev Sci Instrum*. 2006;77(4):041101.

256. Rajan V, Varghese B, van Leeuwen TG, Steenbergen W. Review of methodological developments in laser Doppler flowmetry. *Lasers Med Sci*. 2009;24(2):269-283.

257. Imaging Won R. Mapping blood flow. *Nat Photonics*. 2011;5(7):393.

258. Senarathna J, Rege A, Li N, Thakor NV. Laser speckle contrast imaging: theory, instrumentation and applications. *IEEE Rev Biomed Eng*. 2013;6:99-110.

259. Zeller-Plumhoff B, Roose T, Clough GF, Schneider P. Image-based modelling of skeletal muscle oxygenation. *J R Soc Interface*. 2017;14(127):20160992.

260. Gnyawali SC, Blum K, Pal D, et al. Retooling laser speckle contrast analysis algorithm to enhance non-invasive high resolution laser speckle functional imaging of cutaneous microcirculation. *Sci Rep*. 2017;7:41048.

261. Campbell KR, Chaudhary R, Handel JM, Patankar MS, Campagnola PJ. Polarization-resolved second harmonic generation imaging of human ovarian cancer. *J Biomed Optics*. 2018;23(6):066501.

262. Campagnola P. Second harmonic generation imaging microscopy: applications to diseases diagnostics. *Anal Chem*. 2011;83(9):3224-3231.

263. Cox G, Sheppard CJR. Practical limits of resolution in confocal and non-linear microscopy. *Microsc Res Tech*. 2004;63(1):18-22.

264. Vuillemin N, Mahou P, Débarre D, et al. Efficient second-harmonic imaging of collagen in histological slides using Bessel beam excitation. *Sci Rep*. 2016;6:29863.

265. Bueno JM, Ávila FJ, Artal P. Comparison of second harmonic microscopy images of collagen-based ocular tissues with 800 and 1045 nm. *Biomed Opt Express*. 2017;8(11):5065-5074.

266. Fujimoto JG. Optical coherence tomography for ultrahigh resolution in vivo imaging. *Nat Biotechnol*. 2003;21(11):1361-1367.

267. Mazlin V, Xiao P, Dalimier E, et al. In vivo imaging through the entire thickness of human cornea by full-field optical coherence tomography. In: Ophthalmic Technologies XXVIII. Vol. 10474. International Society for Optics and Photonics; 2018:104740S. https://www.spiedigitallibrary.org/conference-proceedings-of-spie/10474/104740S/In-vivo-imaging-through-the-entire-thickness-of-human-cornea/10.1117/12.2288947.short. Accessed July 30, 2018.

268. de Amorim Garcia Filho CA, Yehoshua Z, Gregori G, Puliafito CA, Rosenfeld PJ. Optical coherence tomography. In: Ryan SJ, Sadda SR, Hinton DR, Schachat AP, Sadda SR, Wilkinson CP, Wiedemann P, Schachat AP, eds. *Retina*, 5th edn. London: W.B. Saunders; 2013:82-110.

269. Tan ACS, Tan GS, Denniston AK, et al. An overview of the clinical applications of optical coherence tomography angiography. *Eye*. 2018;32(2):262-286.

270. Watanabe S, Punge A, Hollopeter G, et al. Protein localization in electron micrographs using fluorescence nanoscopy. *Nat Methods*. 2011;8(1):80-84.

271. Wu R, Zhan Q, Liu H, Wen X, Wang B, He S. Optical depletion mechanism of upconverting luminescence and its potential for multiphoton STED-like microscopy. *Opt Express*. 2015;23(25):32401.

272. Ramachandra R, de Jonge N. Optimized deconvolution for maximum axial resolution in three-dimensional aberration-corrected scanning transmission electron microscopy. *Microsc Microanal*. 2012;18(1):218-228.

273. Trépout S, Bastin P, Marco S. Preparation and observation of thick biological samples by scanning transmission electron tomography. *J Vis Exp*. 2017;121:e55215.

274. Kanemaru T, Hirata K, Takasu S, et al. A fluorescence scanning electron microscope. *Ultramicroscopy*. 2009;109(4):344-349.

275. Reynaud EG, Kržič U, Greger K, Stelzer EHK. Light sheet-based fluorescence microscopy: more dimensions, more photons, and less photodamage. *HFSP J*. 2008;2(5):266-275.

276. Colombelli J, Lorenzo C. Light sheet fluorescence microscopy applications for multicellular systems. In: Cornea A, Conn PM,

eds. *Fluorescence Microscopy*. Boston, MA: Academic Press; 2014:109-120.

277. Doukas CN, Maglogiannis I, Chatziioannou AA. Computer-supported angiogenesis quantification using image analysis and statistical averaging. *IEEE Trans Inf Technol Biomed*. 2008;12(5):650-657.

278. Vickerman MB, Keith PA, McKay TL, et al. VESGEN 2D: automated, user-interactive software for quantification and mapping of angiogenic and lymphangiogenic trees and networks. *Anat Rec*. 2009;292(3):320-332.

279. Palachanis D, Szabó A, Merks RMH. Particle-based simulation of ellipse-shaped particle aggregation as a model for vascular network formation. *Comput Part Mech*. 2015;2(4):371-379.

280. Walpole J, Mac Gabhann F, Peirce SM, Chappell JC. Agent-based computational model of retinal angiogenesis simulates microvascular network morphology as a function of pericyte coverage. *Microcirculation (New York, N.Y.: 1994)*. 2017;24(8); https://doi.org/10.1111/micc.12393.

281. Shirinifard A, Gens JS, Zaitlen BL, Popławski NJ, Swat M, Glazier JA. 3D multi-cell simulation of tumor growth and angiogenesis. *PLoS ONE*. 2009;4(10); e7190.

282. Macklin P, McDougall S, Anderson ARA, Chaplain MAJ, Cristini V, Lowengrub J. Multiscale modelling and nonlinear simulation of vascular tumour growth. *J Math Biol*. 2009;58(4–5):765-798.

283. Kleinstreuer N, Dix D, Rountree M, et al. A computational model predicting disruption of blood vessel development. *PLoS Comput Biol*. 2013;9(4):e1002996.

284. Norton K-A, Popel AS. Effects of endothelial cell proliferation and migration rates in a computational model of sprouting angiogenesis. *Sci Rep*. 2016;6:36992.

285. Moreira-Soares M, Coimbra R, Rebelo L, Carvalho J, D M Travasso R. Angiogenic factors produced by hypoxic cells are a leading driver of anastomoses in sprouting angiogenesis–a computational study. *Sci Rep*. 2018;8:8726.

286. Travasso RDM, Corvera Poiré E, Castro M, Rodrguez-Manzaneque JC, Hernández-Machado A. Tumor angiogenesis and vascular patterning: a mathematical model. *PLoS ONE*. 2011;6(5):e19989.

287. Vilanova G, Colominas I, Gomez H. Coupling of discrete random walks and continuous modeling for three-dimensional tumor-induced angiogenesis. *Comput Mech*. 2014;53(3):449-464.

288. Vilanova G, Colominas I, Gomez H. A mathematical model of tumour angiogenesis: growth, regression and regrowth. *J R Soc Interface*. 2017;14(126):20160918.

289. Guerra MMDSQ, Travasso RDM. Novel approach to vascular network modeling in 3D. In: 2012 IEEE 2nd Portuguese Meeting in Bioengineering (ENBENG); 2012:1-6.

290. Secomb TW, Alberding JP, Hsu R, Dewhirst MW, Pries AR. Angiogenesis: an adaptive dynamic biological patterning problem. *PLoS Comput Biol*. 2013;9(3):e1002983.

291. Santagiuliana R, Ferrari M, Schrefler BA. Simulation of angiogenesis in a multiphase tumor growth model. *Comput Methods Appl Mech Eng*. 2016;304:197-216.

292. Soltani M, Chen P. Numerical modeling of interstitial fluid flow coupled with blood flow through a remodeled solid tumor microvascular network. *PLoS ONE*. 2013;8(6):e67025.

SUPPORTING INFORMATION

Additional supporting information may be found online in the Supporting Information section at the end of the article.